Werk

Jahr: 1981
Kollektion: fid.geo
Signatur: 8 Z NAT 2148:50
Digitalisiert: Niedersächsische Staats- und Universitätsbibliothek Göttingen
Werk Id: PPN1015067948_0050
PURL: http://resolver.sub.uni-goettingen.de/purl?PPN1015067948_0050

LOG Id: LOG_0026
LOG Titel: Calibration of the middle triassic time scale by conventional K-Ar and $^{40}Ar/^{39}Ar$ dating of alkali feldspars
LOG Typ: article

Übergeordnetes Werk

Werk Id: PPN1015067948
PURL: http://resolver.sub.uni-goettingen.de/purl?PPN1015067948
OPAC: http://opac.sub.uni-goettingen.de/DB=1/PPN?PPN=1015067948

Contact

Niedersächsische Staats- und Universitätsbibliothek Göttingen
Georg-August-Universität Göttingen
Platz der Göttinger Sieben 1
37073 Göttingen
Germany
Email: gdz@sub.uni-goettingen.de

J Geophys (1981) 50: 73–88

Journal of Geophysics

Calibration of the Middle Triassic Time Scale by Conventional K–Ar and $^{40}Ar/^{39}Ar$ Dating of Alkali Feldspars

K.N. Hellmann and H.J. Lippolt
Laboratorium für Geochronologie der Ruprecht-Karls-Universität,
Im Neuenheimer Feld 234, D-6900 Heidelberg, Federal Republic of Germany

Abstract. Potassium-argon age determinations were made on 30 alkali feldspar samples from Middle Triassic bentonites of the "Grenzbitumenzone" of Monte San Giorgio (Ticino, Switzerland) which is stratigraphically well-defined by mollusc faunas. The feldspars are of primary volcanic origin (high sanidine) and of secondary authigenic origin (pure K-feldspar with low obliquity). The reported data were determined on the basis of samples from different vertical and horizontal positions within the rock sequence. The high sanidine has been dated at 233 ± 9 m.y., the authigenic feldspar at 226 ± 9 m.y. (IUGS constants, 1977). Stepwise heating experiments using the $^{40}Ar/^{39}Ar$ technique yield well-defined plateaus for the sanidine samples and support the former results. For various reasons the sanidines are thought to be originally volcanic and their K–Ar ages to be the age of eruption. Since the sediments of the Grenzbitumenzone were deposited close to the Anisian-Ladinian boundary, the high sanidine age can be used as calibration point for the Triassic time scale. An extrapolation based on biostratigraphic arguments favors a value close to 250 m.y. for the Permian-Triassic boundary.

Key words: Potassium-argon dating – $^{40}Ar/^{39}Ar$ dating – Triassic time scale – Grenzbitumenzone – Bentonite – Sanidine – Authigenic feldspar – X-Ray diffraction – Neutron activation-Ticino, Switzerland

Introduction

Dating on the Phanerozoic time scale is conducted on the basis of cross-calibration between paleontological correlations and isotopic data. Useful time-marking fossils for the Mesozoic are ammonoids which are cosmopolitan and have a high phylogenetic variability. Obviously, the definition of reliable chronometric calibration points requires thorough paleontological research above as well as below the object to be dated. Therefore, marine ash beds interbedded in fossiliferous sediments offer the best prerequisites for calibrating the fossil-based geological time scale.

Nevertheless, isotopic dating of volcanogenic sediments is often complicated by secondary rebedding, detrital contamination and/or secondary mineralization causing remobilization. Moreover, most submarine ash deposits are affected by halmyrolysis causing devitrification and argon loss. Therefore, potassium bearing minerals with high argon retentivity are the most useful minerals for potassium-argon dating.

Thus, the conditions which the material used for isotopic age determinations and for the definition of calibration points on the biostratigraphic time scale must fulfil, can be summarized as follows:

1. the geological object to be dated should be extracted from primary and stratiform beds between fossiliferous strata of definite stratigraphic positions.
2. different components of the material used for dating must be clearly separable from detrital constituents.
3. there must be various cogenetic minerals of primary origin datable by different methods.
4. the material must be a closed system of radioactive and radiogenic isotopes.
5. the measured age must correspond to the real age of primary crystallization and thus correlate with the biostratigraphic age.

The aim of this study was to define a new calibration point on the Phanerozoic time scale which is significant in relation to biostratigraphic dating as well as to the experimental results. The lack of reliable age data suitable as calibration points for the Mesozoic made efforts in this direction quite challenging.

The Middle Triassic volcanisms of the Southern Calcareous Alps best fulfil the above-mentioned conditions. This is particularly the case for the Anisian-Ladinian boundary in Ticino, Switzerland. There are two reasons for giving preference to this region:

1. the stratigraphic position of the so-called "Grenzbitumenzone" (Frauenfelder 1916) is exactly defined by mollusc faunas.
2. the rock sequence contains volcanogenic intercalations (bentonites) already investigated from sedimentologic and petrographic aspects (Müller et al. 1964).

Among the phenocrysts in the bentonites only high temperature alkali feldspars are suitable for isotopic dating.

Geological Setting

The Mediterranean part of the Tethian geosyncline is characterized by intensive volcanic phases during the Permo-triassic and the Tertiary periods. Figure 1 compiles occurrences of Triassic volcanic rocks in the Mediterranean region which at first were considered candidates for our study. By the evaluation of rock qualities and trustworthiness of their stratigraphic correlation we came to the opinion that the area of this study (D1 in Fig. 1) was most favourable. All the other occurrences of Mesozoic volcanic or intrusive rocks disappointed us as far as their correlation with the geological time scale and/or the mineralogical environment were concerned.

0340-062X/81/0050/0073/$03.20

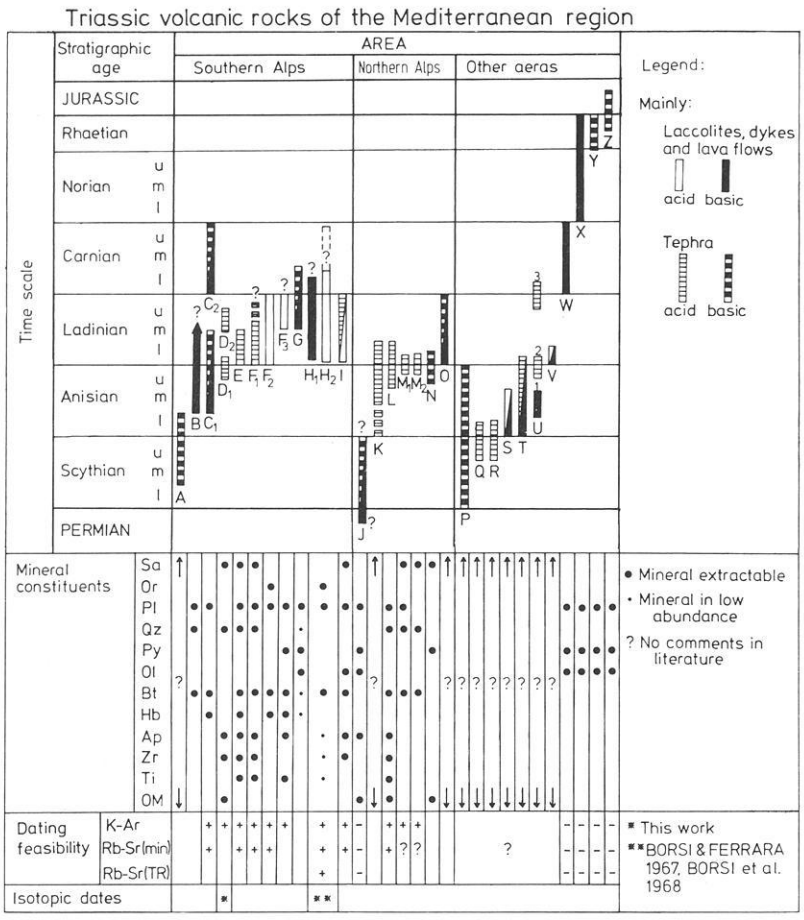

Fig. 1. Stratigraphic comparison of Triassic volcanic rocks in the Mediterranean region and evaluation of their dating feasibility. Rocks of column D_1 were chosen for this study. The notations A to Z stand for: *A* Loibl-Paß, Gartnerkofel (Kahler and Kahler 1953), *B* Valle del Dezzo, Lombardy (Assereto and Casati 1965), C_1 Malpensata/M. Guglielmo, C_2 Val Sabbia (Bianchi et al. 1971), D_1, D_2 Varesotto area (Müller et al. 1964; Wirz 1945), *E* Eastern Dolomites (Caprile, Marmolada, Val Gardena, Latemar (Baccele and Sacerdoti 1965; Callegari and De Pieri 1967), F_{1-3} Recoaro – Schio – Posina area, Vicentinian Alps (Hummel 1931; Zanettin and De Vecchi 1968; Ott 1972; Assereto 1969; De Vecchi et al. 1974), *G* Western Dolomites (Hummel 1932; Rossi 1962; Sacerdoti and Sommavilla 1962), H_1, H_2 Predazzo (H_2)-Monzoni (H_1) area (+intrusive rocks) (Paganelli and Tiburtini 1964; Vardabasso 1945; Simboli 1966; Delmonte 1967; Borsi and Ferrara 1967; Borsi et al. 1968; Gallitelli and Simboli 1970), *I* Carnian Alps (Tarvisiano) (Spadea 1970; Castellarin and Pisa 1974; Assereto et al. 1968), *J* Salzkammergut/Hallstatt (Cornelius 1936, 1941; Zirkl 1957), *K* Schneeberg area, Mieminger mountains, Rhätikon, Wetterstein massive, Lechtal, Karwendel (Spengler and Stiny 1931; Cornelius 1951; Schmidegg 1951; H. Miller 1965; Kobel 1969), *L* Bavarian Alps (Vidal 1953), M_1 Großreifling/Styria, Innsbruck/Austria (Höller 1963; Plöchinger and Wieseneder 1965; Gessner 1966; Summesberger and Wagner 1972; Bechstädt and Mostler 1974), M_2 Göstling/Ybbs, Austria (Faupl and Hamedani 1972), *N* Dobratsch, Gailtal/Austria (Pilger and Schönenberg 1958), *O* Lechtal/Austria (Mutschlechner 1954), *P* NW Bulgaria (Ganev in Zapfe 1974), *Q* Chios/Eastern Aegaeic (Bender 1970; Assereto 1974; Jacobshagen and Tietze in Zapfe 1974), *R* Kithaeron mountains/N-Attika, Greece (Bender 1967), *S* Vilajets Skutari/Albania (Nopcsa and Reinhard 1912), *T* Carpathians, Montenegro (Ramovs in Zapfe 1974; Kuthan 1959), *U* Bükk mountains, Balaton, Bagolyhegy, Hungary (Balogh in Zapfe 1974), *V* Slovenia (Ramovs in Zapfe 1974), *W* Pyrenees (Misch 1934), *X* Keltiberian mountains (Richter and Teichmüller 1933), *Y* Calcena/Moncayo, Arcos de las Salines, Spain (Dubar 1925), *Z* Eastern Pyrenees (Dubar 1925)

In Ticino (Swiss Southern Alps) stratigraphically well-defined volcanic rocks occur. In the region of Lugano there are thin layers of bentonites (altered volcanogenic ejecta) interbedded in a series of fossiliferous bituminous dolostones and argillaceous shales. The fossil record relates this sequence to the Anisian-Ladinian boundary and has therefore been called the "Grenzbitumenzone" (GBZ, "bituminous boundary layer") by Frauenfelder (1916). Outcrops of the GBZ are mainly confined to the area of Monte San Giorgio, south of Lake Lugano.

Seen geologically the Monte San Giorgio area is a fault block, flat-dipping to the south (20–30°), consisting of unfolded conformable beds with a total thickness of more than 800 m from Lower Triassic up to Jurassic, resting concordantly upon various Permian rocks (Fig. 2b).

The GBZ close to the Anisian-Ladinian boundary is a rhythmic alternation of early diagenetic dolomitized limestones and bitumenous shales (± 12 m thickness) conformably interstratified between the laying massive Anisian dolomite and the hanging Ladinian Meride limestone. During the excavation of Middle Triassic vertebrates from 1950–1968 (Kuhn-Schnyder 1964; 1974) the GBZ profile was mapped by paleontologists from Zurich. They divided the whole sequence into layers (nos. 1–180), six of which were recognized as volcanic sediments.

Relation of the "Grenzbitumenzone" to the Triassic Zonal Successions

The Monte San Giorgio area is famous for its abundant deposits of Middle Triassic marine fishes and reptiles (Kuhn-Schnyder 1964). The exact chronostratigraphic position of the GBZ, how-

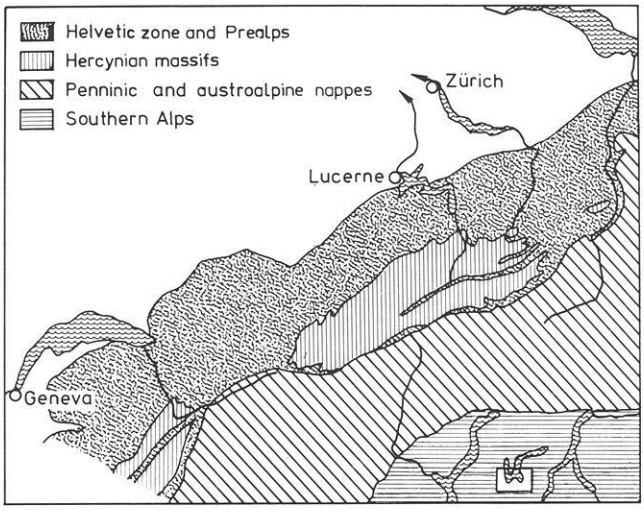

a: Location of sampling area

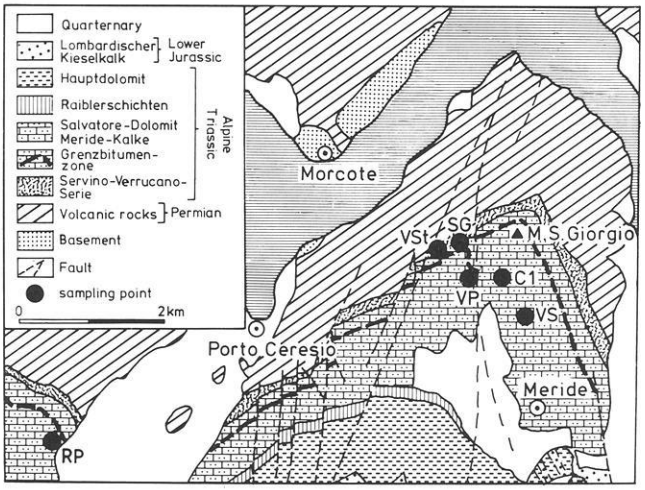

b: Sampling area and sample locations

Fig. 2. a Location (rectangle on the lower right side) and **b** geological sketch of the sampling area in the Monte San Giorgio region south of Lake Lugano (Ticino, Switzerland)

ever, is defined by mollusc faunas (several ammonoid genera; Rieber, 1973b). In the twenties it was already known that the GBZ fauna belongs to a Middle Triassic interval close to the Anisian-Ladinian boundary (Frauenfelder 1916; Senn 1924).

In this context we have to recall what is known about the stratigraphic significance of the GBZ, expecially taking into account the results of the research done at the Mirigioli outcrop of Monte San Giorgio (SG in Fig. 2b; point 902 on folio 1973 Mendrisio 1:25000).

Within the excavated section 44 species and subspecies of 15 ammonoid genera and 12 *Daonella* species (lamellibranchiata of the family Halobiidae) have been found (Rieber 1969, 1973a). The small time range of these fossils permits a highly accurate resolution of the GBZ strata.

The ammonoids are abundant mainly in the dolostone beds of the lower and middle part of the GBZ. Among them Ceratitidae are clearly preponderant. Trachyceratidae are frequent in some beds of the upper part of the sequence. The genus *Protrachyceras Mojsisovics* makes its first appearance in bed no. 98 of the section (compare Fig. 3) thus establishing the lower limit of the Ladinian between bed no. 97 and bed no. 98. Based on Daonellae, the Anisian-Ladinian boundary would coincide with the interval between bed no. 83 and bed no. 104 of the Mirigioli outcrop (Rieber 1969). Comparable Daonella faunas are known from profiles of the Tridentinian Alps and the Dolomites in Southern Tyrol belonging to the latest Anisian and earliest Ladinian.

The Triassic chronostratigraphy, however, is defined only by the zonal succession of ammonoids. Ammonoids are remarkably cosmopolitan and therefore they are of great use for correlating Triassic rocks worldwide (Tozer 1971). Genera of six families of sub-order Ceratitina which are found at Monte San Giorgio are also represented in the Middle Triassic of North America (Silberling and Tozer 1968).

Figure 4 shows the relation of the GBZ to the standard zonal successions of the Alpine-Mediterranean and the North American Triassic. Taking into account the greatest possible error, the GBZ definitely lies above of the Mediterranean *Paraceratites trinodosus* zone and below the *Protrachyceras curionii* zone, which are the middle of *Gymnotoceras meeki* zone and the base of *Protrachyceras subasperum* zone of North America respectively. This corresponds to an interval of two faunal zones. The latest Anisian of the GBZ is characterized by a new faunal

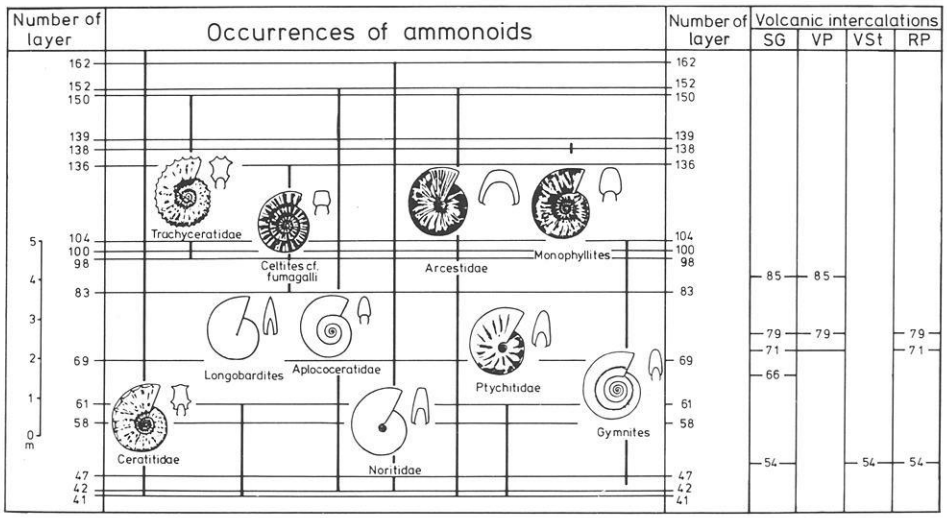

Fig. 3. Occurrence, range and subdivision of stratigraphically significant ammonoids in the Monte San Giorgio limestones (Rieber 1973b) combined with the sequence of bentonites at various outcrops of the area. The numbers characterize the stratigraphic position of fossils and volcanic layers. (SG Mirigioli outcrop, VP Val Porina mine gallery, VSt Valle Stelle gorge, RP quarry near Rossago/Pogliana)

	STAGES	SUBSTAGES	ZONES Alpine-Mediterranean Triassic (ASSERETO1966,69,71)	Grenzbitumen-Zone (RIEBER1969,71,73)	ZONES North America (Silberling & Tozer 1968)	
LADINIAN	UPPER	Longobard	Protrachyceras archelaus		Frankites sutherlandi Maclearnoceras maclearni Meginoceras meginae	
	LOWER	Fassan	Protrachyceras curionii (Protrachyceras reitzi)		Progonoceratites poseidon Protrachyceras subasperum	D.cf.taramellii
ANISIAN	UPPER	Illyr	Aplococeras avisianus Paraceratites trinodosus	Ticinites polymorph.	Gymnotoceras occidentalis Gymnotoceras meeki Gymnotoceras rotelliformis	Daonella dubia Daonella moussoni D.cf.elongata Daonella sturi Daonella americana
	MIDDLE	Pelson	(Balatonites-Horizon)		Balatonites shoshonensis	
		Bithyn	Anagymnotoceras ismidicus		Anagymnotoceras varium	
	LOWER	Aege	(Paracrocordiceras-beds)		Lenotropites caurus	

The chronostratigraphic position of the "Grenzbitumenzone" , dated by ammonoids (Ceratitidae, Hungaritidae , Aplococeratidae, Trachyceratidae) compared with the revised zonal sequence of the Alpine Mediterranean Triassic (left side) and the standard zones of North America (right side)

Fig. 4. Relation of the "Grenzbitumenzone" of Monte San Giorgio to the standard zone succesion of the Alpine-Mediterranean (*left*) and the North American Triassic (*right*)

zone, the zone of *Ticinites polymorphus* RIEBER. This zone may be partly equivalent to the *Aplococeras avisianus* zone defined by Assereto (1969) in the Southern Alpine Triassic taking into account the faunal content. The definition of the upper limit of the *polymorphus* zone in Fig. 4, column 4 (dashed line) as coinciding with the Anisian-Ladinian boundary of the Alpine-Mediterranean succession is justified by the fact that bed no. 98 contains the first Trachyceratidae represented by the genus *Protrachyceras*. Rieber (1973a) considers the layers above bed no. 97 to belong to the *reitzi* zone, eventhough *Protrachyceras reitzi* has not been found. This means that the GBZ also includes the lower part of the Fassan substage, which is indicated by the top line in Fig. 4, column 4. Admittedly, Kozur (1974) doubts that genus *Protrachyceras* appears isochronously on a global scale. He pointed out that this fossil already occurs within the *avisianus* zone. This could mean that the GBZ is really confined to the upper part of the *Aplococeras avisianus* zone and therefore to the latest Anisian. According to Kozur (1974), Silberling & Tozer (1968) have not taken into account representatives of *P. reitzi* when they defined the Anisian-Ladinian boundary because the significant development of genus *Protrachyceras* does not begin until the *P. subasperum* zone.

To sum up briefly we can say that the GBZ is definitely younger than the *trinodosus* zone, older than, or possibly isochronous with the *reitzi* zone of the Alpine standard succession and probably of the same age as parts of the *meeki* and *occidentalis* zone of the North American zonal succession. This implies that the GBZ was sedimented during an interval which lasted as long as one or may be two zones. The exact stratigraphic position therefore may have an error of ± one zone. Assuming that the 34 Triassic zones of more or less the same zonal range have lasted 40–50 m.y., the stratigraphic error is in the order of 1.2–1.6 m.y. This, however, lies within the experimental errors of chronometric dating.

Composition of the Tuffs from the Grenzbitumenzone and Its Implications

The volcanogenic beds are intercalated within the lower to middle part of the GBZ (from bed nos. 29–85) and consist of pure tuffs altered to bentonites without any detrital admixture. The thickness of the layers varies considerably (from a few mm up to several cm). The base of the bentonite beds are often crystal tuff layers, the thickness of which depends on the thickness of the bentonites. This may be due to silica migration resulting from the alteration of the tuffs during diagenetic processes. The volcanic material consists of a micro-crystalline groundmass of illite-montmorillonite composition which contains a small portion of intratelluric phenocrysts of alkali feldspar, quartz and, in some layers, leached euhedral biotite. Euhedral crystals of zircon and apatite are accessory components. Plagioclase, however, is lacking in all horizons. This absence of plagioclase may be an original feature but later alteration into montmorillonite by halmyrolysis cannot be excluded (Helgeson 1972; Wirsching 1976).

The phenocrysts are normally fragments of euhedral crystals with grain sizes less than 1 mm. They amount to ±5% of the samples. The groundmass fraction (less than 2 μm) consists of a mixed-layer mineral of montmorillonite and illite (Müller et al. 1964). The volcanic layers show graded bedding which explains their tuffogenic origin. The mainly splintery, sharp-edged to euhedral phenocrysts, their random distribution in the beds and the lack of detrital compounds are features of aeolic transport followed by sedimentation in the Tethis Sea. Secondary transport and reworking can be excluded.

Sample Val Serrata (VS in Fig. 2b) of our study is stratigraphically younger than the GBZ (from the base up to Lower Ladinian). Contrary to the other samples, it is a tuffite in the sense that it is solidified by calcareous cement. Its origin may

be very similar to the genesis of the GBZ bentonites since it contains quartz and feldspar phenocrysts in graded bedding but no detrital constituents.

Since feldspar turned out to be the only mineral in these tuffs which could be used for dating, we were confronted with the difficulty that only K–Ar measurements could be carried out. Since the Rb/Sr ratio of these feldspars is around 2 (Rb ~ 100 ppm, Sr ~ 50 ppm), Rb/Sr dating would have been possible if a second mineral of volcanic origin had been present in sufficient amounts to permit its separation and the analysis of the initial $^{87}Sr/^{86}Sr$ ratio. Unfortunately the apatite in the tuff samples did not meet this requirement.

Because no second supporting dating method could be applied in this case, we were forced to look for other criteria to check the internal consistency of our dating study. We therefore carefully sampled the material for the K–Ar measurements. This implied a detailed examination of the feldspar types in the tuffs on the one hand, and the preparation of different grain size fractions from those samples from which enough feldspar could be extracted on the other hand. As a further approach we decided not only to apply the conventional K–Ar dating method but also $^{40}Ar/^{39}Ar$ dating with stepwise heating.

Remarks on K–Ar Dating of Feldspar

Müller et al. (1964) have shown that feldspars contained in the bentonites of Monte San Giorgio are only alkali feldspars. As we shall show later the alkali feldspars are sanidine and adularia-like potassium feldspars which may be of authigenic origin. The use of alkali feldspar for K–Ar dating is not unequivocal. Orthoclase and microcline are normally not considered suitable because they obviously do not retain argon as well as sanidine and anorthoclase (compare Dalrymple and Lanphere, 1969, pp 168–170). In general, K–Ar ages will only be geologically meaningful if the object to be dated has initially been free of radiogenic argon and has remained a closed system for argon and potassium since its crystallization.

In the case of the binary system of alkali feldspar the closed system condition can be affected by subsolidus transformations. They are caused by a rearrangement of Si and Al atoms within the lattice in the course of slow cooling of the rocks (diffusive transformation; Laves 1960) and by exsolution or separation of the binary system into sodium and potassium phases.

Random distribution of Al and Si within the lattice of high alkali feldspars is only preserved by rapid quenching near 1,000° C (Stewart and Wright 1974). Long term annealing at temperatures below 800° C causes the aluminium to migrate to electrostatically preferable $T_1(0)$ sites. Because of this the crystal structure becomes more and more triclinic. Only rapid cooling of a melt produces monoclinic potassium rich alkali feldspar of high sanidine structure with maximum Al, Si disorder.

In the course of slow cooling the high sanidine structure will be affected by formation of triclinic domains which produces an apparent integrated monoclinic structure characteristic of "orthoclase" (low sanidine), or it will break down to microcline with maximum Al, Si order, often accompanied by separation of potassium and sodium phases.

The usefulness of high sanidine as a K–Ar clock has long since been established by many authors (Byström-Asklund et al. 1961, Baadsgaard and Dodson 1964; and others). Argon diffusion experiments in a vaccum could be interpreted by simple diffusion mechanisms (Baadsgaard et al. 1961; Frechen and Lippolt 1965; compare Kalbitzer and Fechtig 1966 for general discussion). The argon activation energies are comparable to those of biotites (57 Kcal/mol for the Kinnekulle bentonite sanidine, for instance). The K–Ar results on orthoclase and microcline are confusing. Some data agree quite well with those of cogenetic biotite and hornblende, others not. It is not possible to predict a priori that orthoclase and microcline will yield inconsistent K–Ar results. Perthitization (Sardarov 1957) and obliquity play an important role. The patterns of argon diffusion rates in microcline are quite complicated (Evernden et al. 1960). Low Ar activation energies may be simulated by Ar diffusion from internal surfaces caused by perthitization (Gentner and Kley 1957).

On the contrary, homogeneous orthoclase shows an Ar diffusion pattern comparable to that of sanidine and an activation energy of 44 Kcal/mole (Foland 1974a, b). Na and K diffusion experiments suggest in the case of homogeneous orthoclase and of high sanidine that Ar diffusion maintly takes place on lattice sites of alkali ions, whereas in the case of inhomogeneous orthoclase, triclinic domains are also affected by surface diffusion effects.

The influence of triclinic domains on Ar retentivity has been studied on the basis of $^{40}Ar/^{39}Ar$ stepwise heating experiments of adularias with different obliquities (Halliday and Mitchell 1976). Saddle-shaped $^{40}Ar/^{39}Ar$ spectra were observed, while feldspar with obliquity equal zero yield nearly model release patterns for undisturbed K–Ar systems (rhyolite sanidine, measured by Dalrymple and Lanphere 1974).

In summary we may conclude that the Monte San Giorgio bentonites provide suitable dating material, whereas other feldspar types cannot be considered suitable as long as they have not been tested systematically.

Little is known about the Ar retentivity of authigenic alkali feldspar formed at surface p,T conditions. Most of them have triclinic symmetry. Monoclinic crystals are only found growing on primarily existing nuclei of detritic origin (Füchtbauer 1950, Kastner 1971). Since subsolidus and solvus reactions in authigenic feldspar can be excluded, argon loss is not expected a priori. For an Upper Jurassic tuff from the Southern Alps, Hunziker (1979) found K – Ar ages of sanidines with authigenic K-feldspar rims, which scatter between 136 and 100 m.y., depending on the relative amounts of rim and core analysed. Hunziker assumes on the basis of investigations by Bernoulli and Peters (1974) that the authigenic feldspar rims are products of a later devitrification of the tuff. A value of about 100 m.y. can be derived as devitrification date. This result has to be kept in mind when discussing our results on a presumably authigenic feldspar phase. In case the authigenic feldspar was formed at nearly the same time as the tuff deposition of the bentonite no substantial effect on the ages can be expected. However, if we are dealing with devitrification taking place much later than the formation of the volcanic layers, $^{40}Ar/^{39}Ar$ stepwise heating experiments could be of help in distinguishing between the formation of core and rim.

Sampling and Dressing Procedures

Samples were taken from five sediment outcrops belonging to the GBZ (SG, RP, Vst, VP in Fig. 2b). In addition, material was used from the excavation at Cassina (C1, Lower Ladinian) and from the tuffite within the Lower Meride Limestone of Val Serrata (VS, Lower Ladinian, 100 m above the GBZ). Sample C1, however, did not contain any datable minerals.

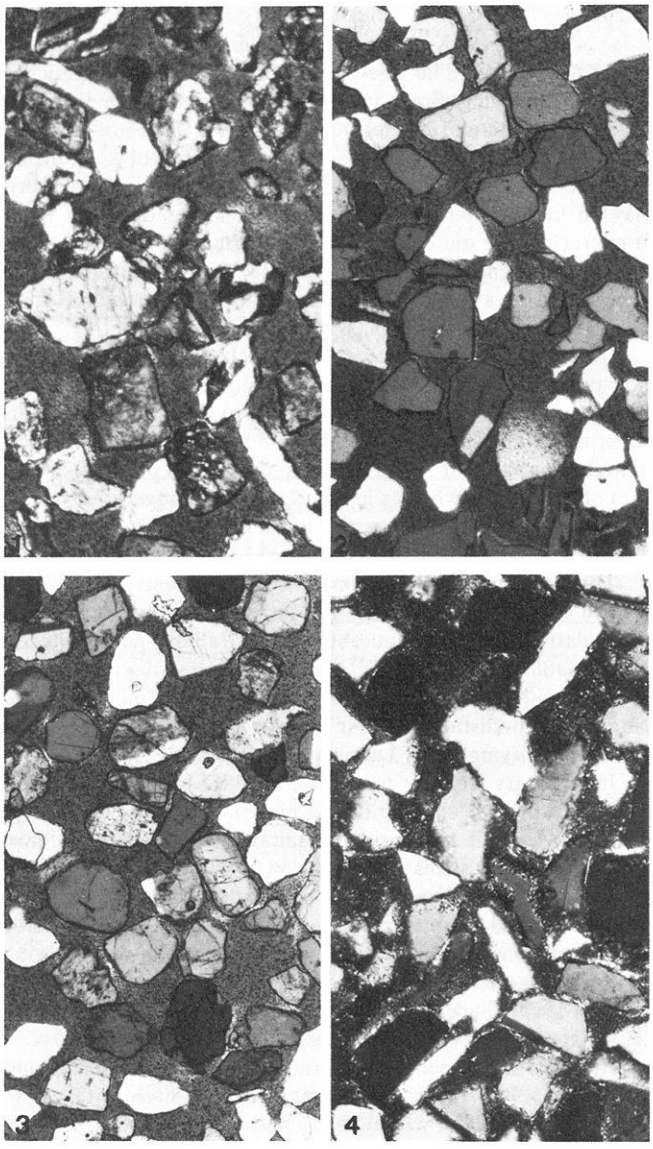

Fig. 5. Photomicrographs of four feldspar concentrates from the bentonite of bed no. 79 at the Mirigioli outcrop (Monte San Giorgio). Grain sizes 200–315 μm, 315–500 μm in Fig. 5-3. *1* Authigenic K feld spar showing inhomogeneous extinction and beginning caolinization (type W in Figs. 6 and 9), *2* clear high sanidine, poor in inclusions (type G), *3* round-edged, cloudy sanidine with inclusions (type R), *4* Sharp-edged, cloudy sanidine of high sanidine quality with overgrowth of authigenic feldspar (type T)

We selected five horizons of the Mirigioli outcrop (SG) and one horizon of the other GBZ outcrops in such a way that three horizons (54, 79, 85) are represented by two independently taken specimens. In total nine different samples were processed. The original samples weighed 20 to 50 kg.

The preparation of the mineral concentrates was begun by decomposing the rocks with suitable solutions, (benzine, hydrogen peroxide) which do not attack the minerals selected for dating. After this treatment the decomposed samples consisted mainly of phenocrysts in their original habit. They were washed several times in twice-distilled water and sieved into five grain size fractions. The fractions 0.1–0.2 mm, 0.2–0.315 mm and 0.315–0.5 mm were chosen for further dressing work. After drying the phenocryst concentrates the feldspars were separated by heavy liquids and magnetic separation. The remaining minerals were examined under the binocular microscope for further datable constituents, however without success. Detrital compounds have not been found in any of the mineral concentrates.

Table 1. Samples of volcanic feldspar prepared from Grenzbitumenzone bentonites and a Lower Ladinian tuffite (VS) of the Monte San Giorgio area, Ticino, Switzerland. (G, W, T: feldspar types described in the text, M mixtures of the three types)

Grain size (μm)	Feldspar types			
	M	G	T	W
100–200	–	–	–	SG 66
	SG 71	–	–	–
	SG 79	SG 79	SG 79	SG 79
	–	RP 79	–	–
	–	VP 85	VP 85	–
200–315	–	–	–	SG 66
	SG 79	SG 79	SG 79	SG 79
	–	–	–	RP 79
	–	SG 85	–	–
	–	VS	–	–
315–500	–	–	–	SG 66
	SG 79	SG 79	SG 79	SG 79
	–	VP 85	VP 85	VP 85
500–1,000	–	VP 85	–	–

The feldspars are alkali feldspars. Optical and morphological differences were observed among the feldspar crystals. On the basis of these differences three feldspar types could be distinguished:

1. A splintery, hypidiomorphic, homogeneous and water-clear type, called "G" (compare Fig. 5, no. 2)
2. A cloudy, partly round-edged type, called "T" (Fig. 5 no. 4)
3. An optically inhomogeneous, hypidiomorphic up to euhedral feldspar type, rich in inclusions, called "W" (Fig. 5, no. 1).

Since a detrital provenience of the round-edged feldspar type "T" could not be excluded a priori, we decided to aim for pure concentrates of the different types, apart from the feldspar mixtures (symbol "M", Fig. 5, no. 3). The selection of the different feldspar types could only be done by handpicking grain by grain. The degree of sample purity reached in this manner was better than 95%. The residual 5% consisted of the two other feldspar types. Each feldspar concentrate was treated with ultrasonics till no further crushing of mineral grains was detectable. The samples were dried and divided into aliquots for different investigations. Each aliquot was examined again under the microscope for its composition. This procedure resulted in a sample reservoir of about 2 g, representing 26 different feldspar samples from seven sampling sites. Bed 54 of the Mirigioli outcrop (SG) and of the Valle Stelle hollow did not contain feldspar; only quartz and montmorillonite were found. Table 1 summarizes the final state of our sample dressing. The majority of the samples consists of the various types and grain sizes of the Mirigioli bentonites 79 and 85.

Experimentation and Results

Structural Examination by X-Ray Diffraction

The structure of the different feldspar types extracted from the tuffs were identified with powdered aliquots using the Phillips X-ray diffractometer of the Mineralogical Institute of the Univer-

Table 2. Certain lines of X-ray diffraction scans (Cu Kα 1) from different feldspar types from Monte San Giorgio bentonites

Reflections (*hkl*)	Feldspar type	
	G and T 2 θ (°)	W 2 θ (°)
($\bar{2}$01)	21.26 ± 0.01	20.96 ± 0.02
(111)	22.67 ± 0.01	22.51 ± 0.02
(130)	23.60 ± 0.01	23.50 ± 0.02
($\bar{1}$12)	25.74 ± 0.02	25.71 ± 0.02
(220)	27.14 ± 0.02	26.81 ± 0.02
($\bar{2}$02)	27.29 ± 0.02	27.11 ± 0.03
(040)	27.38 ± 0.02	–
(002)	27.66 ± 0.01	27.60 ± 0.02
(131)	29.94 ± 0.01	29.81 ± 0.02
(041)	30.76 ± 0.02	30.78 ± 0.02
($\bar{1}$32)	32.36 ± 0.02	32.35 ± 0.02
($\bar{2}$41)	34.94 ± 0.02	34.72 ± 0.02
(060)	41.60 ± 0.01	41.63 ± 0.02
($\bar{2}$04)	50.88 ± 0.01	50.80 ± 0.03
(280)	62.00 ± 0.01	62.01

sity of Heidelberg. Scans were run repeatedly between 65° and 5° at a speed of 1/4° (2θ) per min (time constant position 4). Si metal added to each smear mount was used as an internal standard. The reflections selected for spacing were evaluated in accordance with Orville (1967) and identified on the basis of the powder patterns developed by Wright and Stewart (1968).

The most important 2θ angles are given in Table 2. In this connection the following features must be noted:

1. the pertinent reflections appear at the same angles for the feldspar types G and T, but at significantly different angles for type W.
2. the d-values based on the ($\bar{2}$01) reflections are comparable for all types, within the experimental error, to those reported earlier by Müller et al. (1964) for the tuffogenic feldspar of the Monte San Giorgio.
3. the (130) and (131) reflections for feldspar types G and T are sharp single lines without peak broadening. Therefore the presence of a triclinic component can be excluded. Type W however, shows broadened, diffuse peaks caused by lattice inhomogeneities.
4. the Δ2θ ((040)-(002)) value for the feldspars G and T amounts to 0.27° and is close to that for high sanidine (Borg and Smith, 1969). For type W this value could not be determined because of peak broadening.
5. the d-values obtained from the feldspar types G and T are comparable to those from the Drachenfels sanidine, Eifel (ASTM 19-11227, 1967) whereas the d-values from the feldspar type W are similar to adularia from Selkingen, Switzerland (ASTM 19-931, 1966).

Apart from this it should be mentioned that the 20.95°, 2 θ line found in the type W spectrum can also be seen as a small peak near the ($\bar{2}$01) reflection of type T.

Least squares unit-cell refinements were calculated using a computer program which was developed by Nuber started from calculations made by Berdesinski and Nuber (1966). Only single, well-indexed lines of which the 2 θ values did not scatter more than ±0.03° in repeated runs were used. The results are plotted in Fig. 6.

The lattice constants of the water-clear feldspar type G and the cloudy type T do not differ significantly. They correspond to high sanidine. The type W feldspar, however, has lattice constants equal to those of monoclinic authigenic K-feldspar as reported by Baskin (1956, Table 8) within the experimental errors. Because of the diffuse nature of the X-ray reflections for type W, it was not possible to determine whether the lines are actually split. Fine twinning of triclinic domains can result in an apparent monoclinic symmetry (Goldsmith and Laves, 1954). The broad and diffuse peaks may therefore be due to a domain structure resulting from poor crystallographic continuity.

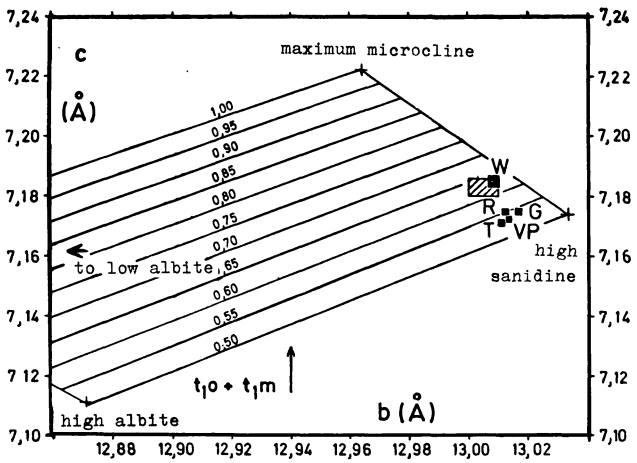

Fig. 6. Lattice parameters of four alkali feldspar types from various bentonite beds of the Monte San Giorgio region (*G*, *VP* clear high sanidine; *T* core of cloudy, sharp-edged high sanidine; *R* round-edged high sanidine; *W* authigenic K-feldspar crystals and rims of T and R). Four samples with nearly complete Al,Si disorder ($T_1 = 0.55$) lie in the high sanidine corner, whereas sample W shows more triclinity ($T_1 = 0.64$). The sizes of the symbols correspond to the analytical errors. The size of the error rectangle for sample W (*cross-hatched*) is due to some diffuse reflections caused by triclinic domains

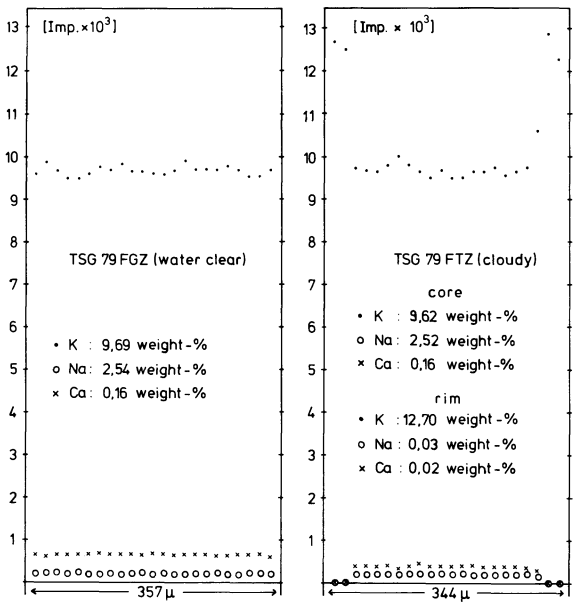

Fig. 7. Concentration profiles of K, Na and Ca across crystals of the feldspar types G (*left*) and T (*right*) showing the overgrowth of the sharp-edged cloudy feldspar crystals. (electron microprobe measurements 15 kV/10 µA, beam diameter 3 µm, integration time 20 s., relative errors ±1%)

Table 3. K–Ar data and ages of volcanogenic and authigenic alkali feldspars of certain grain sizes from one bentonite bed (no. 79) of Mirigioli-outcrop (point 902) at Monte San Giorgio, Ticino (Switzerland). The determined ages of high sanidine and high sanidine with authigenic owergrowths are comparable within the errors

Material analysed	Grain size (mm)	Weight (mg)	K (%)	Rad. ^{40}Ar ($\times 10^{-6}$ cm^3 STP/g)	Atmos. ^{40}Ar (%)	Calculated age (m.y.)
SG 79 type G (primary high sanidine)	0.315–0.500	34	9.95	90.8	3.7	221 ± 7
				91.5	3.5	222 ± 7
	0.315–0.500	44	9.95	96.2	1.5	233 ± 7
				95.6	1.7	232 ± 7
	0.200–0.315	45	9.47	91.8	1.2	234 ± 7
				92.5	1.4	235 ± 8
	0.100–0.200	40	9.27	83.6	1.9	218 ± 7+
				83.9	2.0	219 ± 7+
	0.100–0.200	52	9.27	89.8	0.6	233 ± 7
				89.6	0.8	233 ± 7
					Mean age:	228 ± 7
					Mean age without +:	230 ± 6 (± 11)
SG 79 type T (primary high sanidine with authigenic feldspar rims)	0.315–0.500	39	9.83	93.7	2.2	230 ± 7
				94.9	2.2	233 ± 8
	0.315–0.500	41	9.83	96.8	1.3	237 ± 7
				97.1	1.4	238 ± 8
	0.200–0.315	45	10.07	98.1	1.8	235 ± 7
				98.1	1.8	235 ± 8
	0.100–0.200	39	10.17	99.6	1.7	236 ± 7
				98.9	1.7	234 ± 8
					Mean age:	235 ± 3 (± 6)
SG 79 type W (authigenic K-feldspar)	0.315–0.500	38	12.12	108.7	2.4	217 ± 6
				110.0	2.5	220 ± 7
	0.315–0.500	37	12.12	113.5	1.0	226 ± 7
				113.8	1.1	227 ± 7
	0.200–0.315	44	12.22	115.1	1.5	227 ± 7
				114.7	1.5	227 ± 7
	0.100–0.200	45	11.62	110.0	1.4	229 ± 7
				110.3	1.4	229 ± 7
					Mean age:	225 ± 4 (± 9)
SG 79 type M (three component feldspar mixture)	0.315–0.500	38	10.15	95.2	1.7	226 ± 7
				96.5	1.8	229 ± 7
	0.315–0.500	39	10.15	97.7	3.3	232 ± 7
				97.6	3.3	231 ± 7
	0.315–0.500	39	12.18	116.3	1.8	230 ± 7
				116.8	2.0	231 ± 7
	0.315–0.500	39	10.57	101.1	2.0	231 ± 7
				101.3	2.2	231 ± 7
	0.200–0.315	44	10.16	96.8	1.7	230 ± 7
				96.7	1.9	230 ± 7
	0.100–0.200	44	10.19	98.1	2.1	232 ± 7
				98.2	2.2	232 ± 7
					Mean age:	230 ± 2 (± 4)

Using decay constants $\lambda_e = 0.581 \times 10^{-10} a^{-1}$, $\lambda_\beta = 4.962 \times 10^{-10} a^{-1}$, and atomic abundance $^{40}K/K = 1.167 \times 10^{-4}$
Errors in K = 1.0% (standard deviation of the average on 14 determinations), errors in ^{40}Ar (rad) ± 2.5% per each individual determination. The ± figure is the estimate of precision of the determination at 1 s.d. criterion, 2 s.d. in parentheses

Potassium and Microprobe Analyses

The potassium analyses were carried out by emission flame photometry using a Zeiss spectrometer and applying a modification of Cooper's (1963) method. Standard and sample solutions are buffered with Na and Ca. The measurements are checked by repeated analyses of the NBS 70a standard feldspar, for which Flanagan (1974) recommends 9.80% K as reference. Long time determinations in our laboratory gave 9.78 ± 0.04% potassium (1 s.d. error, 14 values).

Table 4. Conventional K–Ar and $^{40}Ar/^{39}Ar$ total fusion ages on volcanic and authigenic alkali feldspars and feldspar mixtures of certain grain sizes from different bentonite beds of the Mirigioli outcrop (except bentonite bed no. 79) and other localities (sample number corresponds to the number of bentonite bed)

Locality and material analyzed	Grain size (mm)	Weight (mg)	K (%)	Radiogenic ^{40}Ar ($\times 10^{-6}$ cm^3 STP/g)	$^{40}Ar/^{39}Ar$	atm^{40}Ar (%)	Calculated age (m.y.)
loc. Val Serrata (Lower Ladinian) (717.740/084.300, fol. 1373 Mendrisio)							
VS-G (high sanidine)	0.200–0.315	20	–	–	70.477	2.4	227 ± 8
					70.160		226 ± 8
	0.200–0.315	21	–	–	70.477	2.8	223 ± 7
					70.160		223 ± 6
						Mean age:	225 ± 2 (± 4)
loc. Val Porina (716.580/085.300)							
VP 85-G (high sanidine)	0.500–1.000	19	–	–	71.264	2.0	229 ± 8
		12	–	–	70.881	2.3	228 ± 8
	0.315–0.500	40	9.31	89.5		2.0	232 ± 8
				91.1		2.0	236 ± 8
	0.100–0.200	46	9.46	91.6		2.0	233 ± 7
				91.3		2.2	232 ± 8
						Mean age:	232 ± 3 (± 6)
VP 85-T (high sanidine with authig.) feldspar rim	0.315–0.500	43	9.48	88.8		1.6	226 ± 7
				88.5		1.7	225 ± 7
loc. Quarry Rossago/Pogliana (711.100/082.800)							
RP 79-W (authig. K-feldspar)	0.200–0.315	27	13.24	123.4		2.1	225 ± 7
				123.5		2.2	225 ± 7
RP 79-T (high sanidine with authig. feldsp. rims)	0.100–0.200	47	9.85	96.5		1.8	236 ± 7
				96.9		1.9	237 ± 8
loc. Mirigioli (716.512/085.537)							
SG 85-G (high sanidine)	0.200–0.315	10			72.951	4.4	235 ± 15
		11			78.966	6.4	253 ± 11
SG 85-W (authigenic K-feldspar)	0.200–0.315	27	13.24	121.9		2.1	222 ± 3
				122.6		2.3	224 ± 3
SG 71-M (feldspar mixture)	0.100–0.200	65	10.34	95.7		1.4	224 ± 7
				97.0		1.4	227 ± 7
	0.100–0.200	40	10.98	102.5		1.6	225 ± 7
				103.1		1.7	227 ± 7
						Mean age:	226 ± 2 (± 5)
SG 66-W (authigenic K-feldspar)	0.200–0.315	40	13.00	124.1		1.9	230 ± 7
				125.0		2.1	232 ± 7
	0.200–0.315	38	13.00	125.1		0.8	232 ± 7
				124.6		0.9	231 ± 7
	0.100–0.200	45	12.97	121.4		1.1	226 ± 7
				122.4		1.2	228 ± 7
						Mean age:	230 ± 3 (± 5)

The potassium concentrations of the alkali feldspar types of this study are listed in Tables 3 and 4. The data are mean values of duplicate determinations. The concentrations of the three feldspar types W, G and T differ significantly. They are in agreement with the concentrations which can be calculated from the structural properties (section above). Feldspar type W has the highest K content (about 13%), type G 9.5% and type T gave values in between.

Additional measurements have been made by electron microprobe scans. Representative grains of feldspar types G and T were analysed. Figure 7 shows the chemical profiles for the elements K, Na and Ca in the crystals. The water-clear and homogeneous feldspar type G can be distinguished by a homogeneous distribution of the three elements across the crystals, whereas the cloudy feldspar type T exhibits concentration changes towards the rims of the crystal. This suggests that the outer part of this feldspar has a different chemical constitution. The K values increase while the Na and Ca concentrations decrease.

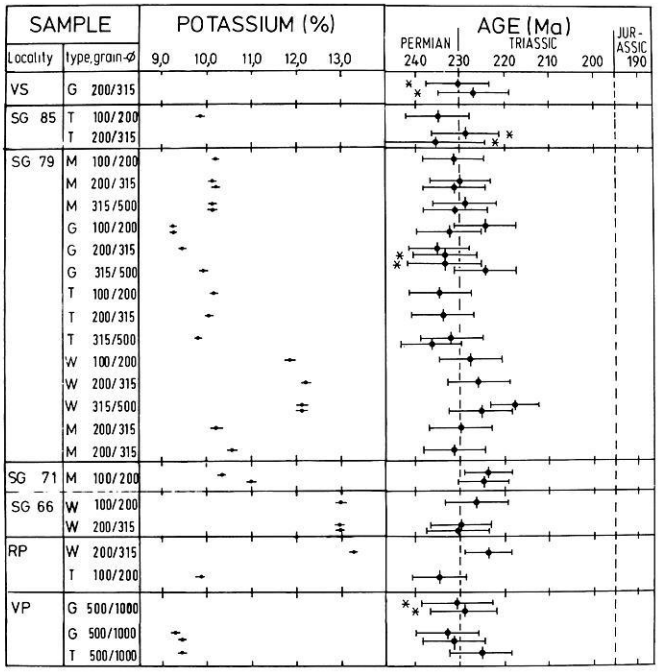

SG = San Giorgio (Mirigioli) ; VP = Val Porina ; VS = Val Serrata ; RP = Rossago/Pogliana
SAMPLE WEIGHTS 40/50 mg; Ar(atm) ~ 2 %
* $^{40}Ar/^{39}Ar$ ages (total fusion); neutron dose ~ $5 \cdot 10^{17}$ n/cm^2

Fig. 8. Potassium contents and K–Ar ages (conventional and $^{39}Ar/^{40}Ar$ total fusion data) of alkali feldspars from different bentonite beds of the Mirigioli outcrop (SG 66, 71, 79, 85) and some other localities (VP, Val Porina, corresponding to SG 85; RP, Rossago-Pogliana, to SG 79; VS, Val Serrata, is already stratigraphically Lower Ladinian)

The intermediate K values of the type T as determined by flame photometry are therefore interpreted as mean values between the concentrations of the core and the rim.

From the Table 3 it can be inferred that the feldspars G and T show systematic K concentration differences according to grain size. Type T has higher values for smaller grain sizes and type G lower values. Both effects are due to admixtures of feldspar with higher K content. In the case of type G the larger grain sizes are richer in this component than the smaller ones; in the case of type T the K-content increases with the decreasing core to rim ratio.

Neutron Activation

Feldspar samples of around 40–50 mg meant for stepwise degassing and samples of around 30 mg for total fusion were neutron irradiated in the reactor of the Nuclear Research Center, Karlsruhe-Linkenheim, West Germany. Sodium-sanidine of the arfvedsonite trachyte from Hohenburg, Siebengebirge (Vieten 1965; Frechen 1976, p14) was used as the irradiation standard. This also serves as the laboratory standard in our dating projects on Tertiary volcanics. The integrated fast neutron dose averaged 5×10^{17} neutrons/cm^2. For irradiation, samples and standards were wrapped in aluminium foil and enclosed in quartz-glass vials. ^{37}Ar was not measured because the low Ca/K ratios of about 1/1000 did not bring about measurable concentrations after radioactive cooling. As standard for the $^{40}Ar/^{39}Ar$ total fusion experiments, we chose sample G (200–315 µm) from bed no. 79 of the Mirigioli outcrop.

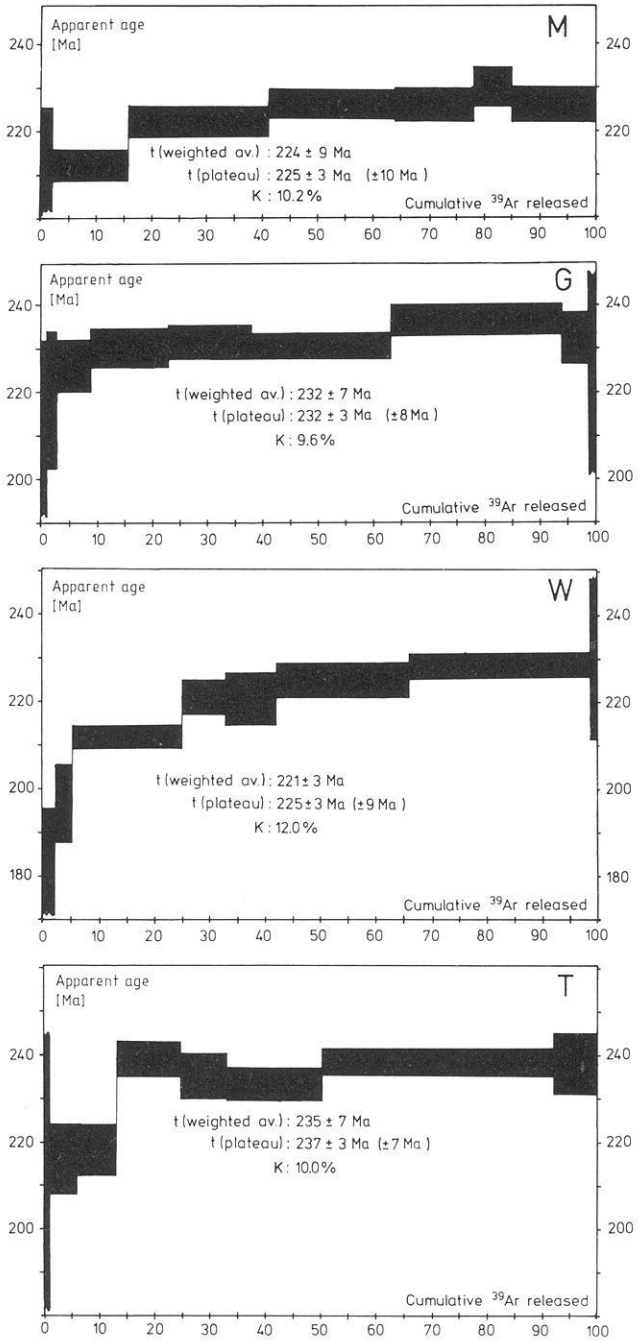

Fig. 9. $^{39}Ar/^{40}Ar$ stepwise degassing plots of three alkali feldspar types found in bentonite SG 79 of the "Grenzbitumenzone" at Monte San Giorgio and of the feldspar mixture (*M*). *W* feldspar with triclinic domains; *T* high sanidine with overgrowth of W, *G* clear high sanidine. Sanidine of the alkali trachyte Hohenburg (Siebengebirge) was used as standard

Argon Analysis

The $^{40}Ar/^{40}K$ measurements were performed between January 1976 and April 1977 (experiment numbers 2330–2885). The $^{40}Ar/^{39}Ar$ analyses were made in July 1976 (step experiments 2596–2601) and May 1977 (total fusion experiments 2906–2937).

The argon isotopes ^{36}Ar, ^{38}Ar, ^{39}Ar and ^{40}Ar were measured on a Varian MAT GD-150 mass spectrometer (180°, 5 cm radius) in static mode, with the accelaration voltage being changed for mass scanning. The total argon blank averaged about

Table 5. Summary of $^{39}Ar/^{40}Ar$ results (step experiments) for feldspar samples W, G, T and M from outcrop Mirigioli (SG 79). Standard: Laboratory standard sanidine Hohenburg, conventional age: 24.9 ± 0.4 m.y.

Sample	Weight (mg)	Run-No.	Steps	^{40}Ar (atm) (%)	Potassium (a) flame phot. (b) ^{39}Ar (%)	(40)/(39) Sample	(40)/(39) Standard	Averaged (A) and Plateau (P) ages (m.y.)
M	39.6	2601	9	5.96	10.17 (12.9)	57.20	6.01 ±0.24	A 223.6 ± 9.0 P 225 ± 3 ± 10
G	40.7	2600	9	3.10	9.56 (10.6)	55.06	5.57 ±0.15	A 231.6 ± 7.0 P 232 ± 3 ± 8
W	38.9	2596	10	4.81	12.99 (11.8)	50.52	5.37 ±0.18	A 221.0 ± 8.0 P 225 ± 3 ± 9
T	44.6	2598	9	4.19	10.02 (8.8)	48.13	4.80 ±0.11	A 235.0 ± 7.0 P 237 ± 3 ± 7

1×10^{-8} cm^3 for the low temperature runs and about 2×10^{-8} cm^3 for the high temperature and fusion runs. The samples were heated and fused by induction heating in molybdenum crucibles. Stepwise heating was started at around 400° C, using nine to ten steps with progressively higher temperatures. The argon was released essentially at around 1,500° C. Prior to the measurements the samples for the conventional isotope dilution analysis (30–50 mg) were preheated at temperatures below 250° C for a duration of about 12 h. The samples for stepwise heating experiments ($^{40}Ar/^{39}Ar$) were preheated at temperatures below 180° C for 24 h. The extracted gases were cleaned by zirconium and titanium getters. The measurements were checked continuously by blank and second degassing runs. Mass spectrometer discrimination was monitored by analysing atmospheric argon quantities comparable to the sample argon.

Decay Constants and Calibrations

The ages were calculated on the basis of the IUGS convention decay constants (Steiger and Jäger 1977). The argon measurements for the K–Ar age determinations were performed in series of eight to ten fusion experiments. Within each series aliquots of the USGS standard biotite LP-6 were measured (Ingamells and Engels 1976; bottles 7-II-C8 and 7-III-D6). During the time devoted to this study forty analyses on this biotite were made. The atmospheric argon contributions were about 5% when using about 50 mg of sample. The standard deviation of the LP-6 measurements was 0.072, or 1.6%. All argon measurements were normalized to an average value of 43.16×10^{-6} cm^3 NTP for LP-6. This argon content corresponds (together with our K value for LP-6 of 8.37%) to an age of 127.8 m.y. Ingamells and Engels (1976) compiled the results of a dozen K–Ar researchers and recommended 43.26×10^{-6} cm^3 as radiogenic argon and 8.325% as potassium concentration (corresponding to an age of 128.9 m.y.). A recent $^{40}Ar/^{39}Ar$ comparison in our laboratory of the micas P-207 and LP-6 (Lippolt et al. 1981) gave 128.6 m.y. for the latter based on 82.6 m.y. for P-207. The degassing spectrum for LP-6 turned out flat with the exception of the first step which showed a higher $^{40}Ar/^{39}Ar$ value than the plateau, similar to the results of Ozima et al. (1979) for LP-6.

Based on the individual errors of the potassium and argon analyses the conventionally determined K–Ar ages in Tables 3 and 4 (measured argon volumes of about 5×10^{-6} cm^3, some percent atmospheric Ar contribution) have standard deviations of about 2% for measurements performed twice and about 3% for single measurements.

The $^{40}Ar/^{39}Ar$ total fusion measurements (Table 4) are based on the K–Ar age of one of the feldspar samples of this study (type G of bentonite 79). This means that they are linked to the calibration described above.

The $^{40}Ar/^{39}Ar$ stepwise heating experiments are calibrated with the K–Ar age of a sanidine from the Siebengebirge (locality Hohenburg). Vieten (1965) and Frechen (1976) give geological and petrographical details. For this sanidine, which for a long time served as our laboratory standard, we used a K–Ar age of 24.9 ± 0.9 m.y. This value is our best estimate for the age of this trachyte, though the long time average is 25.0 m.y. It can therefore not be excluded that the $^{39}Ar/^{40}Ar$ step ages should be higher by 0.4% than given in Table 5 and Fig. 9. The Hohenburg sanidine itself exhibits the degassing pattern of an undisturbed mineral as shown by H.J. Jensen in our laboratory (unpublished). Incomplete melting would therefore not result in severe dating errors. The errors given in Table 5 are standard deviations of the total-argon ages (A) and of the plateau steps (P). As a third value an error estimate for the plateau ages is presented which also comprises the errors of standard calibrations and standard measurements.

Discussion of the Experimental Results

Origin of the Alkali Feldspar Types

The chemical composition of the feldspar phenocrysts from the Monte San Giorgio bentonite based on electron probe measurements can be expressed by the following formulas:

$(K_{0.677}, Na_{0.302}, Ca_{0.021})\ AlSi_3O_8$
$(K_{0.993}, Na_{0.004}, Ca_{0.003})\ AlSi_3O_8$

The first one stands for the type G feldspar and for the core of the cloudy feldspar type T; the latter for the type W feldspar and the rim of type T. The cloudyness of the type T feldspar seems to be due to overgrowth by another feldspar not present in the core. At first we thought we had to distinguish between a sharp-edged and a round-edged cloudy feldspar type, but later on we discovered that the rounding of the feldspar grains might

have been caused by the ultrasonic treatment which partly cleans the T-type feldspar grains from the overgrowth.

The chemical and crystallographic results suggest the existence of two different feldspar phases which originated from two different sources:

a) a high temperature alkali feldspar with a high sanidine structure (G);

b) a low temperature potassium feldspar with poor crystallographic continuity (W).

We have good reason to believe that the high temperature feldspar is of volcanic and the low temperature feldspar is of authigenic origin.

The Authigenic Feldspar: The feldspar considered authigenic has the composition: $Or_{96-98}Ab_{4-2}$ and occurs in all the investigated bentonite beds. The adularia-like habit, the cell dimensions, the chemical composition and the weak Al, Si order are typical for authigenic feldspar. It appears as uniform crystals and as overgrowth on the type G feldspar. According to Baskin (1956) crystallization of potassium feldspar with nearly a stoichiometric composition takes place at temperatures below 100° C. As potassium source we can assume devitrification of rhyolithic glass in a H_2O solvent.

Althaus and Wirsching (1979) showed that the alteration of rhyolithic glass under hydrothermal conditions of 250° C leads to the formation of K feldspar and montmorillonite. The latter mineral can also be formed by alteration of plagioclase. Montmorillonite is a major component of the bentonites. The absence of plagioclase need not be a primary feature, but might be due to this alteration process. Halmyrolytic alteration (devitrification) of submarine ash beds is well known as a potassium source for the formation of new minerals (Füchtbauer 1950; Heim 1960). The authigenic feldspar must be younger than the formation of the bentonite bed. The isotopic age of the feldspar type W therefore could serve only as an age limit for the formation of the Grenzbitumenzone at Monte San Giorgio. Provided that this feldspar type is a retentive K–Ar mineral the isotopic age could give us information on the time of alteration of the sediments. It cannot be excluded that the alteration occurred almost contemporaneously with the deposition.

The Volcanic Feldspar: The feldspar regarded as volcanic has the composition: $Or_{68-69}Ab_{32-31}$ and its occurrence is restricted to the bentonite beds 71, 79 and 85 of our sample reservoir from the GBZ. The water-clear and homogeneous appearance, the high Al,Si-disorder, the cell parameters, and the chemical homogeneity are typical features of crystallization at high temperatures (above 800° C) and of rapid quenching (Ribbe 1975). Obviously there is no reason to doubt the volcanic origin of this feldspar type. It occurs as uniform crystals in type G and as core in the feldspar type T. As the rims of the cloudy feldspar crystals (type T) give reflections different from those of the core, the data points of the water-clear feldspar type G and VP (Fig. 6) from the same bentonite horizon at two different localities and the cloudy type T and R from the locality SG (Fig. 2) cluster close to the high sanidine corner. Whereas the rims of the type T feldspar overlap with the data points of sample W.

The Total Fusion Ages

The total fusion ages of the volcanogenic and authigenic feldspars are compiled in Tables 3 and 4. To facilitate a comparison, figure 8 presents graphically the relations between the samples. Table 3 contains the result obtained from feldspars of bed no. 79 of the Mirigioli outcrop, arranged according to type and grain size. The feldspar data of all other beds of this outcrop and from other localities are given in Table 4 (K–Ar and $^{40}Ar/^{39}Ar$ results).

Since the bentonite from bed no. 79 contains all different feldspar types mentioned above in sufficient concentrations, the argon retention behaviour of the various feldspar types can easily be compared. The ages of the water-clear high sanidine (G: 232 ± 9 m.y. (2 s.d.), 15 analyses) and those of the high-sanidine with overgrowth (T: 235 ± 6 m.y. (2 s.d.), 8 analyses) are the same within the errors, even within 1 s.d. errors. These averages do not include three analyses of the water-clear feldspar which yielded distinctly lower (218 m.y., 219 m.y.) or higher (253 m.y.) ages, though by means of thin section studies no evidence of inhomogeneity or impurities was found. The authigenic feldspar on the average (W: 226 ± 8 m.y. (2 s.d.); 18 analyses) yielded an age, which, even on the 1 s.d. basis, is not significantly lower than the mean age of the volcanic feldspar. For this reason also feldspar mixures (M: 229 ± 5 m.y. (2 s.d.); 16 analyses) with may be 30% W-type feldspar give ages close to those of high sanidine. The results of the cloudy sanidine type (T) indicate that the ages of the high sanidine cores are not seriously affected by the authigenic overgrowths.

The consistency of the age data is satisfactory not only for aliquots of the same sample but also for sample splits with different grain sizes. One may infer from this that there are no crystallographic differences within the spectrum of grain sizes which could have produced a low-retentivity feldspar.

Additionally the data for the sanidines and alkali feldspars from the other bentonite beds of the Mirigioli outcrop (66, 71, 85) and from the corresponding beds of other localities (VP, RP) are consistent with the results of the SG 79 bentonite. The analytical results in Table 4 do not reveal any vertical effect. The ages of sub- and toplayers within the GBZ are concordant within the analytical errors. This is not surprising since the bentonites concerned are not more than 2 m apart. Obviously the sedimentation interval documented by this sequence cannot be resolved by isotopic dating at present. Based on the lifespan of some Daonella species, the accumulation of the 4 m thick rock column could have taken only 1–4 m.y. (Rieber 1969). The Lower Ladinian crystal tuff from Val Serrata, which lies 110 m above the GBZ stratigraphically, yielded a high-sanidine age of 225 ± 4 m.y. From this, for the sedimentation rate, an order-of-magnitude calculation suggests a value of 10 m/m.y. From the data of Tables 3 and 4 an estimate of the interval between formation of the volcanic feldspar and the growth of the authigenic feldspar can be infered. It is probably 23 m.y. at the most and much narrower than in the example described by Hunziker (1979).

The $^{40}Ar/^{39}Ar$ Stepwise Heating Ages

The results of our $^{40}Ar/^{39}Ar$ stepwise heating experiments on the samples SG 79 G, T, W and M are listed in Table 5. In Fig. 9 the individual apparent ages are plotted against the cumulative percentage of released ^{39}Ar. The $^{40}Ar/^{39}Ar$ total argon ages (weighted by means of steps) agree fairly well with the total fusion $^{40}Ar/^{40}K$ ages discussed in the last paragraph. The two differently determined ages (K–Ar; $^{40}Ar/^{39}Ar$) are (2 s.d. errors):

Samples G	232 ± 9 m.y.,	232 ± 14 m.y.
Samples T	235 ± 6 m.y.,	235 ± 14 m.y.
Samples W	226 ± 8 m.y.,	221 ± 16 m.y.
Samples M	229 ± 5 m.y.,	224 ± 18 m.y.

The mean ages of the samples W and M deviate by 4–5 m.y. Again the authigenic feldspar (W) turns out to be younger than the volcanic feldspar represented by samples G and T. All the degassing spectra show a well-developed plateau, but they differ in the first degassing steps.

Sample G behaves as an undisturbed sample. The plateau value is reached after the first two steps which amount to only 3% of the argon released. This behaviour is in accordance with the high argon retentivity of high sanidine.

Sample W, representing the authigenic feldspar, yields a curve which indicates argon loss. After the first three degassing steps (about 23% of the argon) a value of 212 m.y. is reached. From there on it increases slowly to a very narrow plateau value of 225 m.y. (35% of the argon). This plateau value agrees well with the total fusion age. The degassing behaviour of sample W reflects the lower argon retentivity of feldspar with crystal inhomogeneity.

Sample T, sanidine with overgrowth, reaches the plateau value after a 15% ^{39}Ar release. Between the third and the fourth step the $^{40}Ar/^{39}Ar$ ratio increases rapidly, indicating that the core now contributes noticeably to the argon released.

Sample M, which consists of a mixture of the three feldspar types G, W and T (40%, 20%, 40%), reaches the plateau after 40% ^{39}Ar release, but this value is smaller than expected. Actually, the sample may have contained up to 35% weight of feldspar type W, taking into account that the rims of the feldspar grains T are made up of authigenic overgrowth. This does not explain, however, why the plateau value of feldspar types G and T were not reached. It may result from irradiation inhomogeneity or from an underestimation of the type W feldspar component in the mixture. This result may emphasize the importance of using very pure mineral separates, since obviously the individual apparent ages are mineral ages between those of feldspar type G and of feldspar type W.

The results of the $^{40}Ar/^{39}Ar$ step experiments in a $^{40}Ar/^{36}Ar$ versus $^{39}Ar/^{36}Ar$ diagram define straight lines within the analytical errors; the maximum $^{40}Ar/^{36}Ar$ coordinates being 3×10^4–5×10^4. Ages infered from the isochrons agree well with the averages of the steps, either on the basis of all steps or of the plateau steps alone. The intercepts are 290 ± 90 (G), 223 ± 140 (T), 190 ± 192 (W) and 157 ± 190 (M). The relatively high standard deviations of the intercepts are due to the fact that the important steps are very radiogenic and therefore have very high coordinates. The combined plateau – and isochron evaluation shows clearly that the samples are undisturbed in the sense of the four criteria formulated by Lanphere & Dalrymple (1974). The losses of radiogenic ^{40}Ar prior to the analysis amount to about 2% at the most (sample W).

Conclusions

As has been shown, the bentonites intercalated in the Grenzbitumen zone are of volcanic origin and contain high sanidine and authigenic K-feldspar, which are both suitable for K–Ar dating. The total fusion ages of 26 samples (pure sanidine and volcanic feldspar cores) average at 232 ± 9 m.y. (2 s.d.). The authigenic feldspar samples over-all yield an age of 226 ± 8 m.y. (2 s.d.). The combined results of the total fusion (conventionally and $^{39}Ar/^{40}Ar$) and the step degassing experiments are 233 ± 7 m.y. (2 s.d.) for the volcanic feldspar samples and 226 ± 7 m.y. (2 s.d.) for the authigenic feldspar samples. For these averages the plateau ages have been used. When taking into account possible calibration errors the standard deviations increase by 2 m.y. to ±9 m.y.

These results and the well-defined stratigraphic position of the GBZ justify the proposition that this age be used as the new calibration point for the Anisian-Ladinian boundary of the Triassic time scale.

The ages of the high sanidine, however, are about 20 m.y. higher than one would expect on the basis of the Phanerozoic time scale by Harland and Francis (1971). To a certain degree the difference may be due to the new decay constants (Steiger and Jäger 1977), which produce an increase of about 5 m.y. The remaining 15 m.y. are a real discordance and suggest that the Triassic time scale has to be recalibrated.

Furthermore it is evident that the formation of authigenic feldspar can be dated. Because of the lower argon retentivity of this feldspar, the $^{40}Ar/^{39}Ar$ technique is considered a better way to obtain significant results.

Even sanidine with authigenic overgrowth may be of use if the rim/core ratio is favorable. With certain caution the ages obtained for the authigenic feldspar can be considered the age of diagenesis of the Monte San Giorgio rock sequence, especially of the alteration of the tuffs into bentonites. This event took place about 10 m.y. after eruption and deposition of the volcanic material.

As a final remark it should be mentioned that Ferrara and Innocenti (1974) have furnished proof of a thermal event in the Southern Alps which has obviously affected biotite ages of Hercynian basement rocks. This event is thought to be synchronous with the Triassic volcanic phase in this area. As the rocks of our study are sediments and at that time were certainly in a shallow position it is not likely that their volcanic components have been influenced by this event.

Consequences for the Triassic Time Scale

From the well-defined stratigraphic position of the "Grenzbitumenzone" and their bentonites and from the chronometric results of this study we may infer that the Anisian-Ladinian boundary is best dated at 232 m.y. This age is in conflict with the estimates of the currently accepted Triassic time scale according to which the Permian-Triassic boundary would lie close to this age (230 m.y.) and the Anisian-Ladinian boundary at about 210 m.y. These ages are based mainly on K–Ar mineral ages of magmatic rocks from Australia which scatter between 220 and 240 m.y. (Webb and McDougall 1967; Evernden and Richards 1962). Unfortunately the stratigraphic record of these rocks is not really significant and therefore the age data should not be used for time scale calibration. A close look at the more recent publications on the geochronology of Triassic rocks reveals that in fact our result are not in conflict with other information on this subject. Figure 10 summarizes graphically what is known from fifteen papers about isotopic and stratigraphic ages of dated Triassic rocks. The straight line on the left side represents the scale proposed in 1964 (Francis and Harland 1964). It is quite evident that most of the data point to significantly higher values for the Triassic period. The straight line on the right in Fig. 10 represents a calibration line based on more recent data. A more or less similar conclusion has already been drawn by Armstrong and McDowall (1974) and Armstrong (1978). They proposed a value of 212 m.y. for the Triassic-Jurassic boundary and a value of $\geqq247$ and 248 respectively for the Permian-Triassic boundary. Webb (1981), reexamining the available data on the Triassic system, set the boundaries at 200 ± 5 and 245 ± 5 m.y. The calibration point we present here lies right in the straight line on the right side of Fig. 10. Our result is a further proof that the Triassic is confined to an older time

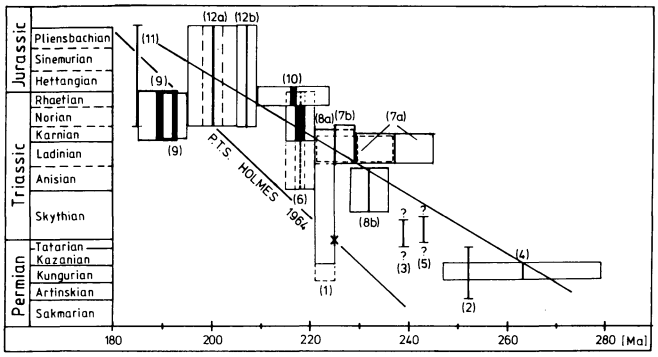

Fig. 10. Relation of isotopic age determinations of Triassic rocks to the pertinent stratigraphic levels. K-decay constants according to Wetherill (1966), Rb-decay constants as proposed by Steiger and Jäger (1977). The K–Ar based rectangles move 2.3% to the right when the IUGS constants are used.
The *numbers* refer to: *1*, *2* Evernden and Richards, 1962, *3* Webb and McDougall, 1967, *4* Kaemmel et al. 1970, *5* Rosenkrantz et al., 1964, *6* Webb and McDougall, 1967, *7a* Borsi and Ferrara, 1967, Borsi et al., 1968, *7b* Borsi et al., 1968, *8* Valencio et al., 1975, *9* Erickson and Kulp, 1961, Fanale and Kulp, 1962, Armstrong and Besancon, 1970. *10* Armstrong and Besancon, 1970, *11* Baadsgaard et al., 1961, *12a* White et al., 1967, *12b* Chrismas et al., 1969. Most ages are K–Ar ages; only 6 (*black box*), 7a and 12b are Rb–Sr results

interval than adopted in 1964, probably between 250 and 210 m.y.

In an earlier discussion Armstrong and Besancon (1970) had assumed that the Triassic period started between 255 and 250 m.y. This estimate was based on an extrapolation using maximum sediment thicknesses of the Triassic. Probably a more reliable extrapolation can be made using the range of ammonoid zones, as the rate of phylogenetic variability is much more sensitive and more time constant than sediment thicknesses. The Anisian-Ladinian boundary divides the 34 ammonoid zones of the Triassic into 16 earlier and 18 later zones. The data of White et al. (1967), Chrismas et al. (1969), Armstrong and Besancon (1970) for uppermost Triassic rocks (205–210 m.y.) and our data allow the calculation of a mean length for a zone in this period (1.2–1.5 m.y.). If we apply the same rate to the sixteen earlier zones, the beginning of the Triassic lies close to 250 m.y.

Acknowledgements. This study was supported by several grants from the Deutsche Forschungsgemeinschaft (project name "Paläovulkanite") for which we are deeply grateful. We are further indebted to the Gesellschaft für Kernforschung, Isotopenstelle, in Karlsruhe-Linkenheim for performing the neutron irradiations. Mr. H. Funke and A. Lutz assisted us with the age determinations, U. Fuhrmann, J. Hess, K. Limbach and M. Hanel with calculations, drawings, etc. This we gratefully acknowledge.

Professor Berdesinski and his co-workers and Dr. B. Nuber helped us to perform the X-ray diffraction work. The electron microprobe analyses were made by Dr. V. Stähle. Professor Kuhn-Schnyder and Professor Rieber (Zürich, Switzerland) gave us considerable advice concerning the Monte San Giorgio paleontological situation. To all of them we would like to express our sincere appreciation.

References

Althaus, E., Wirsching, U.: Experimente zur Bildung von Feldspäten bei der hydrothermalen Umwandlung von Gesteinsgläsern. Fortschr. Mineral. **57**, Beih. 1, I–II, 3–4, 1979

Armstrong, R.L.: Precenozoic phanerozoic time scale – Computer File of critical dates and consequences of new and in Progress Decayconstant revisions. In: 'Contributions to the Geological Time scale', Studies in Geology, No. 6 G.V. Cohee, M.F. Glaessner, H.D. Hedberg, eds.: pp 73–91. Tulsa, Oklahoma, USA: AAPG 1978

Armstrong, R.L., Besancon, J.: A Triassic time scale dilemma: K–Ar dating of Upper Triassic mafic igneous rocks, eastern USA and Canada and post-Upper Triassic plutons, western Idaho, USA. Eclogae Geol. Helv. **63/1**, 15–28, 1970

Armstrong, R.L., McDowall, W.G.: Proposed refinement of the Phanerozoic time scale. Int. Meeting for Geochron., Cosmochron. and Isotope Geol., Paris, 1974

Assereto, R.: Sul ritrovamento di Cefalopodi anisici nella Val Romana (Alpi Giulie occidentali). Riv. Ital. Paleontol. **72**, 3, 591–606, 1966

Assereto, R.: Sul significato stratigrafico della "Zona ad Avisianus" del Trias Medio della Alpi. Boll. Soc. Geol. Ital. **88**, 123–145, 1969

Assereto, R.: Aegean and Bithynian: Proposal for two new Anisian substages. Schriftenr. Erdwiss. Kommiss. Österr. Akad. Wiss. **2**, 23–39, 1974

Assereto, R., Casati, P.: Revisione della stratigrafica permotriassica della Val Camonica meridionale (Lombardia) -Riv. Ital. Paleontol. **71**, 4, 999–1077, 1965

Assereto, R., Desio, A., Di Colbertaldo, D., Passeri, L.D.: Note illustrative della Carta geologica d'Italia alla scala 1:100.000, F^{a}. 14^{A} Tarvisio Serv. Geol. d'Italia, Florenz 1968

ASTM: Spec. Techn. Papers on Powder diffraction standards, compiled by JCPDS, American Soc. Testing materials, Swarthmore, Pennsylvania

Baadsgaard, H., Dodson, M.H.: Potassium-Argon dates of sedimentary and pyroclastic rocks. Quart. J. Geol. Soc. Lond. **120 S**, 119–127, 1964

Baadsgaard, H., Folinsbee, R.E., Lipson, I.: Potassium-Argon dates of biotites from Cordilleran granites. Bull. Geol. Soc. Am. **72**, 689–702, 1961

Baccele, L., Sacerdoti, M.: Una serie di Strati di Livinallongo (Ladinico inferiore) nei pressi di Caprile (Dolomiti Bellunesi). Studi Trent., Sci. Nat. ser. A. **42**, 2, 113–162, 1965

Baskin, Y.: A study of authigenic feldspars J. Geol. **64**, 132–155, 1956

Bechstädt, T., Mostler, H.: Mikrofazies und Mikrofauna mitteltriadischer Beckensedimente der Nördlichen Kalkalpen Tirols. Geol. Paläontol. Mitt. Innsbruck **4**, H. 5/6, 1–74, 1974

Bender, H.: Zur Gliederung der mediterranen Trias II. Die Conodontenchronologie der mediterranen Trias. Ann. Géol. Pays Hélléniques **19**, 465–540, 1967

Bender, H.: Der Nachweis von Unter-Anis ("Hydasp") auf der Insel Chios. Ann. Géol. Pays Hélléniques **19**, 412–467, 1970

Berdesinski, W., Nuber, B.: Vorschlag zur Bestimmung der Bestwerte der Gitterparameter und ihrer Fehlerschranken aus den beobachteten Glanzwinkeln. Neues Jahrb. Mineral. Abh. **104**, 2, 113–146, 1966

Bernoulli, D. & Peters, T.: Traces of rhyolitic-trachitic volcanism in the upper jurassic of the Southern Alps: Reply. Eclogae Geol. Helv. **67/1**, 209–219, 1974

Bianchi, A., Boni, A., Callegari, E., Casati, P., Cassini, G., Comizzoli, G., Dal Piaz, G.B., Desio, A., Guiseppetti, G., Martina, E., Passeri, L.D., Sassi, F.P., Zanettin, B., Zirpoli, G.: Note illustrative della carta geologica d'Italia alla scala 1:100.000, F.^{0} 34 Breno, Serv. Geol. d'Italia, Florenz 1971

Borg, I.Y., Smith, D.K.: Calculated powder patterns. II six potassium feldspars and barium feldspar. Am. Mineral. **54**, 163–181, 1969

Borsi, S. & Ferrara, G.: Determinazione dell' età delle rocce intrusive di Predazzo con i metodi del Rb/Sr e del K/Ar. Mineral. Petrogr. Acta **13**, 45–65, Bologna, 1967

Borsi, S., Paganelli, L. & Simboli, G.: Isotopic age measurements of the M. Monzoni intrusive complex. Mineral. Petrogr. Acta **14**, 171–183, Bologna, 1968

Byström-Asklund, A.M., Baadsgaard, H. and Folinsbee, R.E.: K/Ar age of biotite, sanidine and illite from middle Ordovician bentonites at Kinnekulle, Sweden. Repr. Geol. Föreningens Förhandlingar **83**, H. 1, 92–96, Stockholm, 1961

Callegari, E., De Pieri, R.: Unmixing in the sanidines of the "Pietra

verde" of the Dolomites (Italy). Schweiz. Mineral Petrogr. Mitt. **47**, 1, 111–119, 1967

Castellarin, A., Pisa, G.: Le vulcaniti ladiniche di Forni di Sopra (Carnia occidentale). Mem. Mus. Trid. Sci. Nat. **20**, 99–140, 1974

Chrismas, L., Baadsgaard, H., Folinsbee, R.E., Fritz, P., Krouse, H.R., Sasaki, A.: Rb/Sr, S and O isotope analyses indicating source and date of contact metasomatic copper deposits, Craigmont, British Columbia, Canada. Econ. Geol. **64**, 479–488, 1969

Cooper, J.A.: The flame photometric determination of potassium in geological materials used for potassium argon dating. Geochim. Cosmochim. Acta **27**, 525–546, 1963

Cornelius, H.P.: Eruptivgesteine in den Werfener Schichten der steierisch-niederösterreichischen Kalkalpen. Verh. Geol. B.-A. **10**, 197–202, 1936

Cornelius, H.P.: Zur magmatischen Tätigkeit in der alpidischen Geosynklinale. Ber. Reichsst. Bodenforsch. **1941**, 89–94, 1941

Cornelius, H.P.: Die Geologie des Schneeberg-Gebietes. Jahrb. Geol. Bundesanst., Sonderb. **2**, 115 p., Wien 1951

Dalrymple, G.B.: Critical tables for conversion of K–Ar ages from old to new constants. Geology **7**, 558–560, 1979

Dalrymple, G.B., Lanphere, M.A.: Potassium-argon dating. Principles, techniques and applications to geochronology. San Francisco: Freeman 1969

Dalrymple, G.B., Lanphere, M.A.: $^{40}Ar/^{39}Ar$ age spectra of some undisturbed terrestrial samples. Geochim. Cosmochim. Acta **38**, 5, 715–738, 1974

De Vecchi, G.P., De Zanche, V., Sedea, R.: Osservazioni preliminari sulle manifestazioni magmatiche triassiche nelle Prealpi Venete (Area di Recoaro-Schio-Posina). Boll. Soc. Geol. Ital., 1974

Delmonte, M., Paganelli, L., Simboli, G.: The Monzoni intrusive rocks. A modal and chemical study. Mineral. Petrogr. Acta **13**, 75–118, 1967

Dubar, G.: Etudes sur le Lias des Pyrénées françaises. – Mém. Soc. Géol. Nord **9**, s. 44ff, 214–216, Lille, 1925

Erickson, G.P., Kulp, J.L.: Potassium-argon measurements on the Palisades sill, New Jersey. Bull. Geol. Soc. Am. **72**, 649–652, 1961

Evernden, J.F., Curtis, G.H., Kistler, R.W., Obradovich: Argon diffusion in glauconite, microcline, sanidine, leucite and phlogopite. Am. J. Sci. **258**, 583–604, 1960

Evernden, J.F., Richards, J.R.: Potassium-argon ages in Eastern Australia. J. Geol. Soc. Australia **9**, pt. 1, 1–50, 1962

Fanale, F.P., Kulp, J.L.: The Helium method and the age of the Cornwall Pennsylvania magnetite ore. Econ. Geol. **57**, 735, 1962

Faupl, P., Hamedani, A.: Ein Trachyt-Tuffit aus dem Reiflinger Kalk bei Göstling a.d. Ybbs, Niederösterreich. Mitt. Geol. Ges. Wien **65** (1972), 109–116, 1972

Ferrara, G., Innocenti, F.: Radiometric age evidences of a Triassic thermal event in the Southern Alps. Geol. Rundsch. **63**, 2, 572–581, Stuttgart, 1974

Flanagan, F.S.: Reference samples for the earth sciences. Geochim. Cosmochim. Acta **38**, 1731–1744, 1974

Foland, K.A.. Ar^{40} diffusion in homogenous orthoclase and an interpretation of Ar diffusion in K-feldspars. Geochim. Cosmochim. Acta **38**, 151–166, 1974a

Foland, K.A.: Alkali Diffusion in Orthoclase. In: Geochemical Transport and kinetics ed. Hofmann, A.W. et al., eds.: pp. 77–98, Carnegie Inst. of Washington, publ. 634, 1974b

Francis, E.H., Harland, W.B.: The Phanerozoic time-scale. A symposium dedicated to Professor Arthur Holmes. Quart. J. Geol. Soc. Lond., Vol. 120s (Geological Society Phanerozoic time-scale 1964, pp. 260–262), 1964

Frauenfelder, A.: Beiträge zur Geologie der Tessiner Kalkalpen. Eclogae Geol. Helv. **14**, 2, 247–371, 1916

Frechen, J.: Siebengebirge am Rhein, Laacher Vulkangebiet, Maargebiet der Westeifel. Bornträger, Berlin & Stuttgart, pp. 209, 1976

Frechen, J., Lippolt, H.J.: Kalium-Argon-Daten zum Alter des Laacher Vulkanismus, der Rheinterrassen und der Eiszeiten. Eiszeitalter und Gegenwart **16**, 5–30, Öhringen, 1965

Füchtbauer, H.: Die nicht karbonatischen Bestandteile des Göttinger Muschelkalkes mit besonderer Berücksichtigung der Mineralneubildungen. Heidelberger Beitr. Mineral. Petrogr. **2**, 235–254, 1950

Gallitelli, P., Simboli, G.: Ricerche petrografiche e geochimiche sulle rocce di Predazzo e dei Monzoni (prov. Trento, Italia) svolte nell' Istituto Mineralogica e Petrografica dell' Università di Bologna negli anni 1962–1970. Mineral. Petrogr. Acta **16**, 221–238, 1970

Gentner, W., Kley, W.: Argon-Bestimmungen an Kaliummineralien IV. Die Frage der Argonverluste in Kalifeldspäten und Glimmermineralien. Geochim. Cosmochim. Acta **12**, 323–329, 1957

Gessner, D.: Gliederung der Reiflinger Kalke an der Typlokalität Großreifling an der Enns (Nördl. Kalkalpen). Z. Geol. Ges. **116** (1964), 696–708, 1966

Goldsmith, J.R., Laves, F.: The microline-sanidine stability relations. Geochim. Cosmochim. Acta **5**, 1–19, 1954

Halliday, A.N., Mitchell, I.G.: Structural, K–Ar and ^{40}Ar-^{39}Ar age studies of adularia K-feldspars from Lizard complex, England. Earth Planet. Sci. Lett. **29**, 227–237, 1976

Harland, W.B., Francis, E.H.: The Phanerozoic Time-scale. A Supplement. Geol. Soc. Lond. Spec. Publ. **5**, 356 S., 1971

Helgeson, H.C.: Chemical interaction of feldspars and aqueous solutions. In: The feldspars Mackenzie and Zussmann eds.. pp. 184–217. New York: Manchester Univ. Press, Crane, Russak & Comp., Inc. 1972

Heim, D.: Über die Petrographie und Genese der Tonsteine aus dem Rotliegenden des Saar-Nahe-Gebietes. Beitr. Mineral. Petrogr. 7, 281–317, 1960

Höller, H.: Ein vulkanischer Tuff aus den Reiflinger Kalken, E von Großreifling. Anz. Österr. Akad. Wiss. Math. Natw. Kl. **100**, 323–324, 1963

Hummel, K.: Grünerden Südtirols und sonstige halmyrolythische Eisensilikate. Chemie der Erde. Bd. 6, 469–551, Jena, 1931

Hummel, K.: Oberflächennahe Intrusionen und Trümmerlaven in der südalpinen Mitteltrias. Fortschr. Geol. Paläont. **11**, H. 33 (Deecke Festschr.), 44–74, Berlin, 1932

Hunziker, J.C.: Potassium Argon Dating. In: Lectures in Isotope Geology, E. Jäger, T.C. Hunziker, eds.: 329 pp. Berlin, Heidelberg, New-York: Springer 1979

Ingamells, C.O., Engels, J.C.: Preparation, analysis and sampling constants for a biotite. National Bureau of Standards special publications 422: Accuracy in Trace analysis: Sampling, Sample Handling and Analysis. Proceedings of the 7th IMR Symposium 1976

Kaemmel, T., Pilot, J., Rösler, H.J., Schwab, M.: Radiogeochronologische Daten vom Perm der DDR zur Gewinnung von Eichpunkten für die internationale geochronologische Skala. Z. Angew. Geol. **16**, 2, 57–63, 1970

Kahler, F., Kahler, G.: Das Muschelkalkkonglomerat der Südalpen. Der Karinthin, F. **23**, Klagenfurt, 1953

Kalbitzer, S., Fechtig, H. In: Potassium-Argon Dating (Genter volumn), O.A. Schaeffer, J. Zähringer, eds.. Springer Heidelberg 1966

Kastner, M.: Authigenic feldspars in carbonate rocks. Am. Mineral. **56**, 1403–1442, 1971

Kobel, M.: Lithostratigraphische und sedimentologische Untersuchungen in der kalkalpinen Mitteltrias des Rätikon. Mitt. Geol. Inst., T.H. Zürich, N.F. **118**, 149 p., 1969

Kozur, H.: Probleme der Triasgliederung und Parallelisierung der germanischen und thetyalen Trias, Teil I.: Abgrenzung und Gliederung der Trias. Freib. Forsch. H., **S 298**, 139–197, Leipzig, 1974

Kuhn-Schnyder, E.: Die Wirbeltierfauna der Trias der Tessiner Kalkalpen. Geol. Rdsch. **53**/1, 393–412, 1964

Kuhn-Schnyder, E.: Die Triasfauna der Tessiner Kalkalpen. Neujahrsblatt Nat.-Forsch. Ges. Zürich, 119 S. Zürich: Leemann 1974

Kuthan, M.. Spuren der vulkanischen Tätigkeit in der mittleren Trias des Slowakischen Karstes. Geol. Práce, Zoš. **56**, 55–74, Bratislava, 1959

Lanphere, M.A., Dalrymple, G.B.: Final compilation of K–Ar and Rb–Sr measurements on P-207, the USGS interlaboratory standard muscovite. In: F.J. Flanagan, ed.. Descriptions and analyses of eight new USGS rock standards. Geol. Surv. Prof. Pap. **840**, 127–130, 1976

Lanphere, M.A., Dalrymple, G.B.: The use of $^{40}Ar/^{39}Ar$ data in evaluation of disturbed K–Ar systems, in R.E. Zartman (ed.) Geol. Surv. Open-File report **78–701** (Snowmass colloquium 1978 abstracts), 241–243, Denver, 1978

Laves, F.: Al/Si – Verteilungen, Phasen – Transformationen und Namen der Akalifeldspäte. Z. Kristallogr. **113**, 265–296, 1960

Lippolt, H.J., Raczek, I., Schleicher, H.. Das Isotopenalter ($^{40}Ar/^{39}Ar$; Rb–Sr) eines Autun-Biotits aus der Bohrung Wrzesnia/Polen. Der Aufschluß, im Druck, Jahrgang 1981

Miller, H.. Die Mitteltrias der Mieminger Berge mit Vergleichen zum westlichen Wetterstein-Gebirge. Verh. Geol. B.-A., 187–212, Wien 1965

Misch, P.. Der Bau der mittleren Südpyrenäen. In: Beiträge zur Geologie der westlichen Mediterrangebiete, Nr. 13. Abh. d. Ges. Wiss. Göttingen, math.-phys. Kl. III. Folge, H. 12, 1934

Müller, W., Schmid, R., Vogt, P.: Vulkanogene Lagen aus der Grenzbitumenzone (Mittlere Trias) des Monte San Georgio in den Tessiner Kalkalpen. Eclogae Geol. Helv. **57**, 2, 431–450, 1964

Mutschlechner, G.: Die Massengesteine der Nordtiroler und Voralberger Kalkalpen. T Cherm. Mineral. Petrogr. Mitt. **4**, 386–395, 1954

Nopsca, Baron F., Reinhard, M.: Zur Geologie des Vilajets Skutari in Nordalbanien. An. Ist. Geol. al Românici, 5, Fasc. 1, 1–24. Jb. d. KK. Geol. R.-A. **61**, 2, 1–24, 1912

Orville, P.M.: Unit-cell parameters of the microline-low albite and the sanidine-high albite solid solution series. Am. Mineral. **52**, 55–85, 1967

Ott, E. Die Kalkalgen-Chronologie der alpinen Mitteltrias in Angleichung an die Ammoniten-Chronologie. Neues Jahrb. Geol. Palaeontol. Abh. **141**, 1, 81–115, 1972

Ozima, M., Kaneoka, I., Yanagisawa, M.: Temparature and Pressure Effects On ^{40}Ar-^{39}Ar Systematics. Earth Planet. Sci. Lett. **42**, 463–472, 1979

Paganelli, L., Tiburtini, R. The Predazzo granite (North Italy). Mineral. Petrogr. Acta **10**, 57; 1964

Pilger, A., Schönenberg, R.: Der erste Fund mitteltriadischer Tuffe in den Gailtaler Alpen (Kärnten) Z. Geol. Ges. **110**, 205–215, 1958/59

Plöchinger, B., Wieseneder, H.: Ein Biotitandesit-Tuffit im Reiflinger Kalk des Schwarzkogels bei St. Gallen im Ennstal, O. Österreich. Verh. Geol. Bundesanst. 59–69, 1965

Ribbe, P.H.. The chemistry, structure and nomenclature of feldspars (R-11). In: Feldspar mineralogy, P.H. Ribbe ed. Mineral. Soc. Am., short course notes, **2**, Blacksburg, Virginia: Southern Printing Comp. 1975

Richter, G., Teichmüller, R. Die Entwicklung der Keltiberischen Ketten. Beitr. Geol. westl. Mediterrangebiete Nr. 9 Abh. Ges. Wiss. Göttingen, meth.-phys. Kl., III F., **7**, 1067–1186. Berlin: Weidmann 1933

Rieber, H.. Daonellen aus der Grenzbitumenzone der mittleren Trias des Monte San Georgio (Kt. Tessin, Schweiz). Eclogae Geol. Helv. **62**, 2, 657–683, 1969

Rieber, H. Cephalopoden aus der Grenzbitumenzone (Mittlere Trias) des Monte San Georgio (Kt. Tessin, Schweiz). Schweiz. Palaeontol. Abh. **93**, 1–96, 1973a

Rieber, H.: Ergebnisse paläontol.-stratigraph. Untersuchungen in der Grenzbitumenzone (Mittl. Trias) des Monte San Georgio (Kt. Tessin, Schweiz). Eclogae Geol. Helv. **66**/3, 667–685, 1973b

Rosenkranz, A.A., Semenova, T.P., Monich, V.K., Kovaleva, V.V. The Geochronological data on the upper palaeozoic continental formations in Kazakhstan. XXII. Int. Geol. Congr. Probl. **3**, 172–176, 1964

Rossi, D.: Geologia della parte meridionale del gruppo della Marmolada. Mem. Mus. Storia nat. Venezia Trident, XXV–XXVI, 1962–1963, vol. XIV, Fasc. 1/B., pp. 189, Trento, 1962

Sacerdoti, M., Sommavilla, E.: Pillowlave, jaloclastiti ed altre formazioni vulcanoclastiche nella Regione Dolomitica Occidentale. Studi Trent. Sci. Nat., a. XXXIX, n. 3, 423–473, Trento, 1962

Sardarov, S.S. Retention of radiogenic argon in microline. Geochimistry **3**, 233–237, 1957

Schmidegg, O. Die Stellung der Haller Salzlagerstätte im Bau des Karwendelgebirges. Jahrb. Geol. Bundesanst. **94** (Festband), 159–205, Wien, 1951

Silberling, N.J., Tozer, E.T.: Biostratigrafic classification of the marine Triassic in North America. Geol. Soc. Am. Spec. Pap. **110**, 1–63, 1968

Simboli, G. Ricerche petrochimiche e considerazioni petrologiche sulle formazioni vulcaniche triassiche di Val Gardone (Predazzo). Mineral Petrogr. Acta **12**, 37–60, 1966

Spadea, P.: Le ignimbriti riolitiche del membro superiore delle vulcaniti di Rio Freddo, nel Trias medio della regione di Tarvisio (Alpi Giulie Occidentali). Stud. Trent. Sci. Nat., Sez. A **47**, 2, 287–358, 1970

Spengler, E., Stiny, J.: Erläuterungen zu Blatt Schneeberg, St. Ägyd 1·75000. Geol. Bundesanst. Wien, 1931

Steiger, R.H., Jäger, E.: Subcommission on Geochronology: Convention on the use of decay constants in geo- and cosmochronology. Earth Planet. Sci. Lett. **36**, 359–362, 1977

Stewart, D.B., Wright, T.L.: Al/Si order and symmetry of natural alkali feldspars and the relationship of strained cell parameters to bulk composition. Bull. Soc. Fr. Mineral. Cristallogr. **97**, 356–377, 1974

Summesberger, H., Wagner, L.: Der Stratotypus des Anis (Trias). Annalen Naturhist. Mus. Wien **76**, 515–538, 1972

Tozer, E.T. Triassic time and ammonoids: problems and proposals. Can. J. Earth. Sci. **8**, 989–1031, 1971

Vardabasso, S.: Lo stato attuale delle nostre conoscenze sulla provincia petrografica di Predazzo. Atti. Ist. Veneto di Sci. T CIV, Parte 2ª, Venezia, 1944/1945

Valencio, D.A., Mendia, J.E., Vilas, J.F. Paleomagnetism and K–Ar ages of Triassic igneous rocks from the Ischigualasto-Ischichuca basin and Puesto Viejo formation, Argentinia. Earth Planet. Sci. Lett. **26**, 319–330, 1975

Vidal, H.: Neue Ergebnisse zur Stratigraphie und Tektonik des nordwestlichen Wettersteingebirges und seines nördlichen Vorlandes. Geologica Bavarica **17**, 56–88, 1953

Vieten, K.: Manganreicher Fluotaramit aus dem Alkalitrachyt der Hohenburg bei Berkum (Siebengebirge). Neues Jahrb. Mineral. Monatsh. **6**, 166–171, Stuttgart, 1965

Webb, J.: A radiometric time scale of the Triassic. J. Geol. Soc. Australia **28**, 107–121, 1981

Webb, A.W., McDougall, J. Isotopic dating evidence on the age of the Upper Permian and Middle Triassic. Earth Planet. Sci. Lett. **2**, 483–488, 1967

Wetherill, G.W.: Radioactive decay constants and energies. In: S. Clark (editor) Handbook of Physical constants. Geol. Soc. Am. Mem. **97**, 513–519, 1966

White, W.H., Erickson, G.P., Northcote, K.E., Dirom, G.E., Harakal, J.E.: Isotopic dating of the Guichon batholith, B.C. Can. J. Earth. Sci. **4**, 677–690, 1967

Wirsching, U.: Experimente zur Bildung von Tonmineralien bei der hydrothermalen Umwandlung von Feldspäten. Fortschr. Mineral. **54**, Beih. 1, I–II, 104–105, Stuttgart, 1976

Wirz, A.: Beiträge zur Kenntnis des Ladinikums im Gebiet des Monte San Georgio. Schweiz. Pal. Abh. **65**, 1–84, 1945

Wright, T.L., Stewart, D.B. X-ray and optical study of alkali feldspars: I. Determination of composition and structural state from refined unit-cell parameters and 2 V. Am. Mineral. **53**/1, 38–87, 1968

Zanettin, B., De Vecchi, G.P.. Porfiriti triassiche. In: Note illustrative della Carta geologica d'Italia, Foglio Schio. Serv. Geol. Italia, 1968

Zapfe, H. (Hersg.): Die Stratigraphie der alpin-mediterranen Trias. Schriftenr. Erdwiss. Kommiss. Österr. Akad. Wiss. **2**, 251 p. Wien: Springer 1974

Zirkl, E.J.: Der Melaphyr von Hallstadt. Jahrb. Geol. Bundesanst. **100**, H. 2, 137–178, 1957.

Received January 12, 1981 ; Revised version July 30, 1981
Accepted September 26, 1981